HHS Public Access

Author manuscript

Biochim Biophys Acta Mol Basis Dis. Author manuscript; available in PMC 2023 August 01.

Published in final edited form as:

Biochim Biophys Acta Mol Basis Dis. 2022 November 01; 1868(11): 166515. doi:10.1016/j.bbadis.2022.166515.

The nuclear receptor TLX (NR2E1) inhibits growth and progression of triple- negative breast cancer

Adam T. Nelczyk[1], **Liqian Ma**[1,$], **Anasuya Das Gupta**[1], **Hashni Epa Vidana Gamage**[1], **Michael T. McHenry**[1], **Madeline A. Henn**[1,&], **Mohammed Kadiri**[1], **Yu Wang**[1], **Natalia Krawczynska**[1], **Shruti Bendre**[1], **Sisi He**[1,#], **Sayyed Hamed Shahoei**[1,*], **Zeynep Madak-Erdogan**[2,7,8], **Shih-Hsuan Hsiao**[3], **Tareq Saleh**[4], **Valerie Carpenter**[5,!], **David A. Gewirtz**[5], **Michael J. Spinella**[6,7,10], **Erik R. Nelson**[1,6,7,8,9]

[1]Department of Molecular and Integrative Physiology, University of Illinois Urbana-Champaign, Urbana, Illinois 61801, USA.

[2]Department of Food Science and Human Nutrition, University of Illinois Urbana-Champaign, Urbana, IL 61801, USA

[3]Veterinary Diagnostic Laboratory, College of Veterinary Medicine, University of Illinois Urbana-Champaign, Urbana, Illinois 61801, USA.

[4]Department of Basic Medical Sciences, The Hashemite University, Zarqa, Jordan

[5]Department of Pharmacology and Toxicology, Virginia Commonwealth University, Richmond, Virginia, 23298, USA

[6]Department of Comparative Biosciences, University of Illinois at Urbana-Champaign, Urbana, Illinois, 61801, USA

[7]Cancer Center at Illinois, University of Illinois Urbana-Champaign, Urbana, Illinois 61801, USA.

[8]Division of Nutritional Sciences, University of Illinois Urbana-Champaign, Urbana, Illinois 61801, USA.

[9]University of Illinois Cancer Center, University of Illinois at Chicago, Chicago, Illinois 60612, USA.

[10]Carl R. Woese Institute for Genomic Biology, Anticancer Discovery from Pets to People Theme, University of Illinois Urbana-Champaign, Urbana, Illinois 61801, USA.

Abstract

Development of targeted therapies will be a critical step towards reducing the mortality associated with triple-negative breast cancer (TNBC). To achieve this, we searched for targets that met three criteria: (1) pharmacologically targetable, (2) expressed in TNBC, and (3) expression is prognostic

[$]Current Affiliation: Tempus, Chicago, IL, USA
[&]Current Affiliation: Ann & Robert H. Lurie Children's Hospital of Chicago, Chicago, IL, USA
[#]Current Affiliation: NGM Biopharmaceuticals Inc., South San Francisco, CA, USA
[*]Current Affiliation: Cancer Biology and Genetics Program, Sloan Kettering Institute, Memorial Sloan Kettering Cancer Center, New York, NY, USA
[!]Current Affiliation: Translational Genomics Research Institute, Phoenix AZ, USA

Declaration of Interest statement: The authors have no competing interests or conflicts of interest to declare.

in TNBC patients. Since nuclear receptors have a well-defined ligand-binding domain and are thus highly amenable to small-molecule intervention, we focused on this class of protein. Our analysis identified TLX (NR2E1) as a candidate. Specifically, elevated tumoral TLX expression was associated with prolonged recurrence-free survival and overall survival for breast cancer patients with either estrogen receptor alpha (ERα)-negative or basal-like tumors. Using two TNBC cell lines, we found that stable overexpression of TLX impairs *in vitro* proliferation. RNA-Seq analysis revealed that TLX reduced the expression of genes implicated in epithelial-mesenchymal transition (EMT), a cellular program known to drive metastatic progression. Indeed, TLX overexpression significantly decreased cell migration and invasion, and robustly decreased the metastatic capacity of TNBC cells in murine models. We identify SERPINB2 as a likely mediator of these effects. Taken together, our work indicates that TLX impedes the progression of TNBC. Several ligands have been shown to regulate the transcriptional activity of TLX, providing a framework for the future development of this receptor for therapeutic intervention.

Introduction

Anti-endocrine and anti-HER2 therapies are not indicated for the treatment of patients diagnosed with triple-negative breast cancer (TNBC), as these tumors stain negative for the estrogen receptor alpha (ERα), progesterone receptor and HER2. As the vast majority of TNBC cases fall into the PAM50 basal-like molecular subtype, the terms are often used synonymously. However, TNBC is a highly heterogenic malignancy that does not neatly fit into any one of the molecular subtypes, and in fact consists of at least 6 distinct TNBC subtypes [1]. Current standard of care for TNBC patients generally consists of surgical intervention coupled with radiation therapy and chemotherapeutic compounds such as anthracyclines or taxanes [2]. While these modes of intervention do yield some survival benefits, many of them have considerable side-effects that detract from quality of life [3–6]. Unfortunately, even with the implementation of these therapies, TNBC patients continue to experience higher rates of recurrence and metastasis, and worse overall survival compared to patients with other breast cancer subtypes [7, 8]. Due to this reality, considerable effort has been put into exploration of targeted therapies for TNBC [9–11], which recently culminated in the approval of two new therapies: PARP inhibition (Olaparib) for the treatment of patients with mutations in BRCA1/2, and the use of immune checkpoint inhibitors (anti-PD-L1 and anti-PD-1) in combination with nab-paclitaxel combinatorial therapy [12, 13]. Acquired resistance to PARP inhibition remains a significant clinical challenge. Furthermore, the approval for immune checkpoint blockade was only indicated for patients whose tumors expressed the protein PD-L1, and even in this cohort, the response rate is poor [14, 15]. Genentech has recently announced that it will not be pursuing full FDA approval for its anti PD-L1 therapy for various reasons, leaving only anti-PD-1 available. The poor prognosis and recent developments highlight the need for continued pursuit of targets for the effective treatment of TNBC.

Therefore, we initiated a search for putative targets that met three criteria: (1) pharmacologically targetable, (2) expressed in TNBC, and (3) expression is prognostic in TNBC patients. Nuclear receptors comprise a diverse superfamily of ligand-inducible transcription factors [16]. They all contain a well-defined ligand-binding domain, making

them highly amenable to small-molecule intervention, a feature well-known for the successful targeting of the estrogen, progesterone, androgen and glucocorticoid receptors [17]. The endogenous ligands (if any) for several nuclear receptors have not yet been described. Previous work has identified several nuclear receptors and their prognostic value in breast cancer [18]. We were intrigued by these so-called orphan nuclear receptors, as often synthetic ligands have been developed, but their biology not well described. Therefore, we assessed various nuclear receptors as to whether their tumoral expression was associated with prognosis for patients with ERα-negative and HER2-negative tumors, or TNBC tumors.

In doing so, we identified TLX (Nuclear Receptor Subfamily 2 Group E Member 1, NR2E1), as being associated with a good prognosis in breast cancer patients. TLX has primarily been characterized in neural and retinal progenitor cells as a repressive transcription factor that inhibits expression of tumor suppressor genes, such as cyclin-dependent kinase inhibitor 1A (*CDKN1A*/p21), and phosphatase and tensin homolog (*PTEN*). Thus, through its repression of these tumor suppressors, TLX ultimately facilitates the proliferation of these progenitor cells [19–23]. In line with this biology, several studies focusing on cancers of the brain and prostate describe TLX as a pro-oncogenic factor that can enable enhanced proliferation and invasiveness [24–29]. To date, only one study has been published regarding the role of TLX in breast cancer [30]. Results from this work demonstrated an inverse relationship between TLX and ERα expression, and that acute perturbations of TLX either promoted (overexpression) or inhibited (knockdown) proliferation and invasion *in vitro*. Using a similar approach, we were able to recapitulate these results. However, clinical data presented here indicate that ERα-negative and basal-like patients with higher expression of TLX experienced improved recurrence-free and overall survival. These seemingly paradoxical findings indicated that perhaps transient perturbations of TLX expression was not representative of its physiological functions in the prolonged disease state typically experienced by breast cancer patients. Therefore, we utilized stable overexpression of TLX in TNBC cell lines to more faithfully replicate prolonged perturbations in the levels of TLX likely experienced by patients. Under these conditions, we observed multiple anti-cancer phenotypic and transcriptomic changes, implying the possibility that TLX may play a pro-survival role in certain breast cancer patient populations.

Materials and Methods

Clinical Data Analysis

Data used for analysis of breast cancer patient gene expression and survival was downloaded from the Kaplan-Meier Plotter webtool (https://kmplot.com/analysis/) [31] and cBioPortal (https://www.cbioportal.org/) [32–34]. The Kaplan-Meier Plotter webtool uses aggregated data from GEO, EGA, and TCGA and allows users to restrict breast cancer survival analyses based on features such as hormone status, molecular subtype, tumor grade, and treatment status. It uses univariate and multivariate Cox proportional hazards survival analysis with an algorithm to parse based on gene expression resulting in the most significant difference

between groups [35]. cBioPortal was used to obtain the Breast Invasive Carcinoma (TCGA PanCancer) and Breast Cancer (METABRIC) datasets.

Cell Culture

MDA-MB-231 and luciferase/GFP dual-labeled MDA-MB-468 (# SL027, GeneCopoeia, USA) cells were grown in DMEM supplemented with 10 % FBS (#SH30396.03, HyClone, USA) and 1% penicillin-streptomycin antibiotic mixture (##30–002-CI, Corning, USA). When passaging cells, cells were first washed with DPBS (#17–512-F, Lonza, USA) and then detached with 0.05% trypsin with 0.53 mM EDTA (#24–052-CI, Corning, USA). Cells were authenticated at the Cancer Center at Illinois Tumor Engineering and Phenotyping (TEP) Shared Resources. All cells were tested and found to be negative for mycoplasma contamination. TLX^{+} and TLX^{con} stable cell lines were generated by transfecting cells with either a TLX pcDNA3.1^{+}/C-(K)DYK plasmid (OHu23488, GenScript, USA) or pcDNA3 empty vector (a generous gift from the Donald P McDonnell Lab, Duke University) using lipofectamine 2000 (#11668019, Invitrogen, USA). For MDA-MB-231 cells, after selection with 800 μg/ml G418 Sulfate (#10131035, Gibco, USA), single cell colonies were isolated, and expanded. For MDA-MB-468 cells, after selection with 600 μg/ml G418 Sulfate, a pooled clone approach was used, as these cells were unable to thrive as single cell colonies.

Proliferation

Cells were seeded in 96-well plates (#667196, Dot Scientific Inc., USA) at a density of 200–2,000 cells/well. Proliferation was measured using the DNA stain Hoescht 33342 as previously described [36].

Cell Cycle

Cell cycle progression was assessed following synchronization of cells in G1 phase [37]. Briefly, 10^6 MDA-MB-231 cells were seeded in a 100 mm plate for 24 h, followed by 36 h treatment with 10 μM lovastatin (Tocris Bioscience, UK) to achieve synchronization. Cells were released from G1 synchronization by treatment with 1 mM Mevalonate. Cells were harvested and stained with BD Pharmigen PI/RNase staining buffer (BD Biosciences, USA) following manufacturer protocol. Samples were analyzed using a BD Accuri C6 Flow Cytometer (BD Biosciences, USA) and cell cycle distribution was determined using FCS Express 6 Software (De Novo Software, USA).

Cell Death

For cell death assays, either 0.375×10^6 (6-day assay) or 1.5×10^6 (24 h assay) MDA-MB-231 cells were seeded in 100 mm plates. Each assay included a control plate treated with 2 μM staurosporine to induce cell death. Cells were harvested and stained using the FITC Annexin V/Dead Cell Apoptosis Kit (Invitrogen, USA) following manufacturer protocol. Samples were analyzed using a BD Accuri C6 Flow Cytometer and cell status (live, early apoptotic or dead) was determined using FCS Express 6 Software.

DNA Synthesis

For DNA synthesis assays, MDA-MB-231 cells were seeded in 6-well plates at a density of 0.350×10^6 cells/well for 12 h. Cells were treated with 10 μM EdU for 10 h and then the assays were completed using the Click-iT Plus EdU Alexa Fluor 488 Flow Cytometry Assay Kit (Invitrogen, USA) following manufacturer protocol. Samples were analyzed using a BD Accuri C6 Flow Cytometer and the percent of cells with newly synthesized DNA (successful incorporation of EdU) was determined.

Senescence

MDA-MB-231 cells were seeded in 24-well plates at a density of 2,000 cells/well, with media changes performed every other day. On day 6, cells were treated with either DMSO or 0.5 μM Epirubicin Hydrochloride Alfa Aesar, USA) for 48 h. On day 8, cells were harvested, and protein content (for sample normalization) was analyzed using the Pierce BCA Protein Assay Kit (#23227, Thermo Fisher Scientific, USA). SA-β-galactosidase activity was then assessed using the Cellular Senescence Assay Kit (Cell Biolabs Inc., USA) following manufacturer protocol. Fluorescence signal was determined using a SpectraMax M2 Multi-Mode Microplate Reader (Molecular Devices LLC, USA)

Migration

For migration assays, cells were seeded in 6-well plates at a density of $0.4–0.5 \times 10^6$ cells/well for 24 h. A single scratch was introduced down the center of the well using a p200 pipette tip followed by imaging at 4X magnification using an EVOS XL Digital Inverted Brightfield and Phase Contrast Microscope (Invitrogen, USA) at 8 h intervals for 32 h. Images were analyzed using the ImageJ plugin, Wound Healing Size Tool [38, 39]

Invasion

For invasion assays, 10^6 cells were seeded in 100 mm plates and grown for 24 h in serum-containing media. Cells were then incubated for an additional 24 h in serum-depleted media. Following serum starvation, invasion assays were performed following the CytoSelect 24-well cell invasion assay (basement membrane, fluorometric format) manufacturer protocol (Cell Biolabs Inc., USA). Fluorescence signal was determined using a SpectraMax M2 Multi-Mode Microplate Reader.

RNA Interference

MDA-MB-231 TLX^{con} and TLX^{+} cells were seeded in 6-well plates at a density of $0.3–0.4 \times 10^6$ cells/well for 24 h. Cells were transfected for 48 h with either a universal negative control siRNA (#SIC001, Millipore Sigma, USA), a TLX-targeting siRNA (SASI_Hs01–00210050, Millipore Sigma, USA) or a SERPINB2-targeting siRNA (SASI_Hs01_00120712, Millipore Sigma, USA) using DharmaFECT 4 Transfection Reagent (Horizon Discovery LTD, UK). TLX-targeting 1 siRNA sequence: 5’-UAGAGUGUUAGCAUCAACC-3’ TLX-targeting 3 siRNA sequence: 5’-AAAGCGACAGGGUUGAGUG-3’ SERPINB2-targeting siRNA sequence: 5’-UUCUCCCUGUCAUAACACC-3’

Real-time quantitative polymerase chain reaction (qPCR)

RNA extraction from cell lysate and mouse tissue, cDNA synthesis, and gene expression analysis were done as previously described [36, 40]. TBP was used as a housekeeping gene. TBP forward primer: 5'-TGCCCGAAACGCCGAATATA-3'. TBP reverse primer: 5'-TTCTTGCTGCCAGTCTGGAC-3'. TLX forward primer: 5'-AATGGGCCATTCCGGTTGAT-3'. TLX reverse primer: 5'-AATCGAGCCACCACCTCTTG-3'. SERPINB2 forward primer: 5'-TCTCAGAGGAGCATTGCCCG-3'. SERPINB2 reverse primer: 5'-GATCCTCCATTGTTTCAATCTGGT-3'.

RNA sequencing and data processing

MDA-MB-231 TLX^{con} and TLX^{+} cells were seeded and treated as described in the RNA interference section. RNA extraction was performed using the RNeasy Plus Mini Kit (#74136, Qiagen, Germany). Samples were analyzed at the Roy J. Carver Biotechnology Center at the University of Illinois at Urbana-Champaign. RNA quality and concentration were confirmed using an AATI Fragment Analyzer (Agilent Technologies Inc., USA), and Qubit Fluormeter (Thermo Fisher Scientific, USA) respectively prior to library preparation. Sequencing was done using 100bp single reads in one SP lane of a NovaSeq 6000 (Illumina, USA). Transcript abundance was quantified using Kallisto (v0.44.0) pseudoalignment, using index built from a transcriptome fasta of Homo sapiens build GRCh38 (Ensembl). Transcript abundance scaled by the average transcript length and to library size was subsequently summarized to gene-level counts using R package Tximport. After keeping all the genes that were expressed in at least 1 sample, 27548 genes were left for downstream analysis, and differentially expressed gene analysis was performed using R packages Limma-voom and EdgeR on the logCPM values. False discovery rate (FDR) method was used to correct for multiple testing. PCA plot was generated using the R function prcomp() and ggplot2. Volcano plots were made using GraphPad Prism (Version 8). This data has been deposited into GSE196105 (https://0-www-ncbi-nlm-nih-gov.brum.beds.ac.uk/geo/query/acc.cgi?acc=GSE196105).

Protein Quantification

MDA-MB-231 and MDA-MB-468 TLX^{con} and TLX^{+} cells were seeded in 100 mm plates at a density of $0.75–1 \times 10^{6}$ cells and grown for 24 h. Protein was extracted using either RIPA buffer (#89900, Thermo Fisher Scientific, USA) or M-PER (#78503, Thermo Fisher Scientific, USA) and then quantified using a Pierce BCA Protein Assay kit (#23227, Thermo Fisher Scientific, USA). Protein was run on SDS-PAGE for western blot analysis, and TLX protein was detected using the anti-NR2E1 antibody (#ab109179, Abcam, USA). Anti-cyclophilin B antibody (#sc-517566, Santa Cruz Biotechnology, USA) was used as an internal control. Blot images were acquired using the iBright CL1000 (#A32747, Invitrogen, USA) and protein levels were quantified either using Image Studio Lite Version 5.2 (LI-COR Biosciences, USA) or iBright Analysis Software Version 5.0.0.

TLX Gene Signature

Data from our RNA-Seq analysis as well as the available patient data from METABRIC was used to make the downregulated and upregulated TLX signature. The comparisons in this data were set up as follows: siCont-TLX^{+} to siCont-TLX^{con} and siTLX-TLX^{+} to siCont-TLX^{+}. From these two lists, all gene expression changes that had an FDR < 0.01 were retained for further analysis. From these two lists, we selected genes that showed a 2-fold or greater change in expression (downregulation or upregulation). We further narrowed down these lists by parsing out the genes that did not appear in both comparisons. Additionally, as the two comparisons are inverted (overexpression vs control and knockdown vs overexpression) we parsed out any genes whose expression changes (downregulated or upregulated) were not opposite between the two comparisons. The final downregulated and upregulated gene signature lists only included the genes for which METABRIC patient data was available (117 downregulated genes and 11 upregulated genes). For the two different signatures, patient signature scores were derived by combining the Z-scores of all the genes for a given patient. Patients were then parsed into high (top 25%) and low (bottom 25%) cohorts and their survival data was assessed using Kaplan-Meier analysis.

Gene Set Enrichment Analysis

Using the data from our RNA-Seq analysis, gene set enrichment analysis (GSEA) was done using the Broad Institute GSEA software (Version 4.1.0) and the Hallmark Gene Sets collection from the Molecular Signatures Database (MSigDB v7.3, https://www.gsea-msigdb.org/gsea/msigdb/index.jsp) [41]. The two comparisons for the analysis were as follows: siCont-TLX^{con} to siCont-TLX^{+} and siTLX-TLX^{+} to siCont-TLX^{+}. Gene sets that showed significant enrichment (FDR < 0.05) in both comparisons were selected for further analysis. Specifically, within each gene set, only the genes that were significantly altered across both comparisons were considered potential regulatory targets.

nCounter Gene Profiling

NanoString nCounter SPRINT Profiler using the Breast Cancer 360 Panel was used to analyze RNA isolated from cell lysate and mouse tissues [42]. Alterations in gene expression were analyzed using nSolver (Ver 4.0). Pathway analysis was performed using the PANTHER Classification System (http://www.pantherdb.org/) [43].

Animal Studies

All protocols involving animals were approved by the Institutional Animal Care and Use Committee (IACUC) at the University of Illinois at Urbana-Champaign. Female athymic nude mice were purchased from Charles River Laboratories and female NOD SCID gamma (NSG) mice were purchased from Jackson Laboratory. Mice were housed with ad libitum access to food and water and 12 h light and dark cycles.

In Vivo Primary Tumor Growth.—Athymic nude mice were grafted with either 10^6 TLX^{con} or TLX^{+} (N = 8) MDA-MB-231 cells in the axial mammary gland. Mice were checked for palpable tumors starting 8 days post-graft and every 3 days thereafter until tumors became measurable (14 days post-graft). Mice were euthanized 53 days post-graft

(a single TLX^{con} mouse was euthanized 51 days post-graft due to unexpected weight loss). Tumors were excised from all mice, split, and either snap frozen using liquid nitrogen for RNA analysis or fixed in 10 % formalin for histological staining. The study was repeated independently as follows. Athymic nude mice were grafted with either 10^6 TLX^{con} or TLX^+ MDA-MB-231 cells in the axial mammary gland. Mice were checked for palpable tumors starting 7 days post-graft and every other day thereafter until tumors became measurable (12 days post-graft). This study was originally designed to be part of a larger study, and thus both groups were also treated daily with a placebo (saline) 3 x/week for 21 days, and then at 3 x/week every other week. Mice were euthanized when tumors reached a volume of 1250 mm^3. At 70 days post-graft, all remaining mice were euthanized.

In Vivo Metastatic Colonization (MDA-MB-231).—Athymic nude mice were grafted with 10^6 MDA-MB-231 cells in the lateral tail vein. At the end of the study, lungs were excised from all mice and then briefly inflated using DPBS. Lungs were then split in half, one of which was snap frozen for RNA analysis, and one of which was fixed in 10 % formalin for histological staining.

In Vivo Metastatic Colonization (MDA-MB-468).—NSG mice were grafted with 10^6 luciferase/GFP dual-labeled MDA-MB-468 (# SL027, GeneCopoeia, USA) cells in the lateral tail vein. Mice were imaged via the *in* vivo live imaging system (IVIS) 1 x/week throughout the study. Bioluminescent signal was analyzed using Aura (Ver 4.0) (Spectral Instruments Imaging, USA).

Histopathology and Analysis.—Tumor and lung samples were submitted to the University of Illinois at Urbana-Champaign College of Veterinary Medicine Diagnostic Laboratory for histopathological analysis by a board-certified veterinary pathologist blinded to experimental design and treatment status.

Statistics

Data are expressed as mean ±SEM unless otherwise indicated. Cell culture assays were repeated in at least two independent experiments. Statistical analyses were performed using GraphPad Prism Version 8 unless otherwise indicated. Data was ln-transformed or non-parametric tests were used as appropriate. Comparisons between two groups were analyzed using student's unpaired two-tailed t test, between three or more groups were analyzed using one-way ANOVA followed by Tukey's multiple comparisons test, between two groups through multiple time-points were analyzed using two-way ANOVA followed by Šidák's multiple comparison test. One phase decay nonlinear regression was used to analyze difference in migration between TLX^{con} and TLX^+ cells. Survival data was assessed using Kaplan-Meier analysis followed by the log-rank test and Gehan-Breslow-Wilcoxon test. Significance was determined to be $P \leq 0.05$.

Results

TLX expression is elevated in ERα-negative and basal breast tumors, and is positively correlated with survival

In order to identify potential new targets for the treatment of breast cancers lacking ERα and HER2, we searched for orphan nuclear receptors that had high expression in TNBC and whose tumoral expression was associated with prognosis [either recurrence-free survival (RFS) or overall survival (OS)]. Initial analysis was performed using the Kaplan-Meier Plotter webtool (https://kmplot.com/analysis/) which uses patient data from three different sources: Gene Expression Omnibus (GEO), European Genome-Phenome Archive (EGA), and The Cancer Genome Atlas (TCGA) [31]. In doing so, we found that TLX was generally expressed at higher levels in ERα-negative tumors compared to ERα-positive ones (Fig. 1A). This was confirmed in the METABRIC [34] dataset (Fig. 1B). More comprehensive analysis of the TCGA and METABRIC databases where patient tumors were parsed based on their PAM50 subtype indicated that the basal subtype of TNBC tend to have elevated TLX expression, while the claudin-low TNBC subtype, luminal subtypes and normal subtype had lower expression (Fig. 1C–D). Thus, TLX met our first criteria of being expressed or enriched in the common basal subclass of TNBC. It was next important to determine if its expression was associated with prognosis.

Our initial analysis utilized a feature where data are parsed into groups based on the most significant outcome per query. This analysis revealed that higher expression of TLX was correlated with improved survival (RFS and OS) for both ERα-negative and basal-like breast cancer subgroups, (Fig. 1E–H). When assessing only high-grade tumors (grade 3, poorly differentiated), TLX continued to be associated with improved RFS and OS, indicating that it likely plays important inhibitory roles in disease progression (Fig 1I–L).

To explore these associations in a more stringent manner, we ran a second series of analyses by comparing defined quartile and tertile parameters. Importantly, a positive correlation between TLX and both RFS and OS was observed when comparing the quartile and tertiles for ERα-negative breast cancer patients respectively (Supplemental Fig. 1A–B). Similar results were observed for basal-like breast cancer patients, although they were underpowered to reach statistical significance (Supplemental Fig. 1C–D). Interestingly, no association between TLX and survival was observed for patients with ERα-positive tumors (Supplemental Fig. 1E–F), indicating that either the basal expression of TLX in these tumors is too low to exert effects, or that it plays different roles depending on the subtype. Collectively, these data support a clinically relevant role for TLX in TNBC progression. It was therefore important to use preclinical models to more comprehensively evaluate the impact of TLX on breast cancer pathophysiology.

Chronic overexpression of TLX reduces proliferation of cellular models of TNBC.

TLX is responsible for regulating neural-stem cell proliferation via its repression of targets such as p21 and PTEN [44]. In cancers of the brain and prostate, inhibition of TLX has been shown to impede cancer cell and tumor growth, as reviewed in [44]. Similarly, previous work in breast cancer models indicated that transient overexpression of TLX appeared to

exert a pro-proliferative activity in MDA-MB-231 cells, while transient knockdown of TLX inhibited growth in MDA-MB-157 and MDA-MB-468 cells [30]. We were able to repeat these results in MDA-MB-231 cells where transient overexpression of TLX in this cell line promoted proliferation as observed on day 4 (Fig. 2A). However, we noticed that these effects were diminished or reversed towards the terminal timepoints of our commonly used assay (Fig. 2A). Conversely, siRNA mediated knockdown of TLX in MDA-MB-157 cells that have high basal expression of TLX, had no significant effects on this slow growing line; similar results being obtained with two different targeting siRNAs (Fig. 2B & Supplemental Fig. 2). Therefore, we extended this assay to longer timepoints, and observed that TLX overexpression actually inhibited proliferation over 14d, while siRNA-mediated knockdown resulted in increased proliferation at this timepoint (Fig. 2C–D & Supplemental Fig. 2).

This change in proliferation kinetics through time was intriguing, especially considering the clinical data indicating that TLX was protective (Fig. 1). Transient overexpression and our acute timepoints are unlikely to accurately reflect tumor biology, as breast tumor growth in humans is on a longer timescale than these *in vitro* models, and without other perturbation, tumoral TLX expression would be expected to be stable through time.

Therefore, we elected to investigate the impact of chronically overexpressing TLX levels in two different TNBC cell lines (basal TLX expression in the cell lines used shown in Supplementary Fig. 3A). Stable overexpression resulted in an induction of ~15 and ~3048-fold mRNA expression in in MDA-MB-231 and MDA-MB-468 cells respectively (control and overexpression referred to as TLX^{con} and TLX^{+} forthwith; two clones of MDA-MB-231 cells were generated) (Supplementary Fig. 3B–C, E).

As expected, based on our transient overexpression studies, the MDA-MB-231 TLX^{+} line had decreased proliferative capacity compared to a control clone with an empty vector (TLX^{con}; Fig. 2E). Reduced proliferation was recapitulated in MDA-MB-468 TLX^{+} cells (Fig. 2F, Supplementary Fig. 3D). Thus, similar to the longer timepoints when TLX was acutely overexpressed, chronic overexpression also impaired proliferation, which is likely to be a more physiologically relevant scenario.

To better understand the potential causes of this slowed proliferation, we investigated several cellular processes that TLX may be regulating. Cell death (apoptosis), DNA synthesis and senescence did not appear to account for the observed proliferative deficit in MDA-MB-231 TLX^{+} cells (Supplementary Fig. 4A–D). However, one notable change we observed in MDA-MB-231 TLX^{+} cells was that they would consistently accumulate in the S-phase of the cell cycle, while TLX^{con} cells continued into the G2/M phase (Supplementary Fig. 4E). The lag in cell cycle progression experienced by TLX^{+} cells would carry over into the G2/M phase, while TLX^{con} cells would complete the mitotic process, thereby providing a potential explanation for the proliferative deficit observed in TLX^{+} cells.

TLX alters the MDA-MB-231 transcriptome

As a nuclear receptor, TLX is generally thought to reduce the expression of target genes through the recruitment of histone deacetylases (HDACs) and other co-repressor molecules. To provide insight into the biological function of TLX in TNBC, we performed RNA-Seq

analysis on TLX^{con} and TLX^{+} MDA-MB-231 cells (TLX expression confirmed by qPCR as depicted in Fig 3A). Overexpression of TLX resulted in the differential regulation of 5,967 genes compared to control cells (Fig. 3B–D, GSE196105). Importantly, in order to assess those genes that may be acutely regulated via TLX versus those that may be secondary targets or adaptive responses to chronic overexpression, we included a group of TLX^{+} cells treated with siRNA against TLX (siTLX). Treatment of TLX^{+} cells with siTLX resulted in the differential regulation of 4,589 genes when compared to TLX^{+} cells treated with a control siRNA (siCont) (Fig. 3B–D). Further analysis showed that these two different conditions had 2,277 genes in common that were differentially expressed, and that 1,326 (~58%) were recovered by treatment of TLX^{+} cells with siTLX (Fig. 3B–D). To gain further insight into the likely mechanisms/pathways TLX was impinging on, we performed gene set enrichment analysis (GSEA) using the Hallmark Gene Sets collection [41] on differentially regulated genes when comparing siCont-TLX^{con} to siCont-TLX^{+}, and siTLX-TLX^{+} to siCont-TLX^{+} (Fig. 3E, Supplementary Tables 1 & 2). Our analyses suggest that TLX exerts its repressive effect on several pathways and processes that are well-known to promote the progression of cancer (Fig. 3E–F & Supplementary Fig. 5).

TLX overexpression resulted in the repression of genes that were enriched in two gene sets of particular interest. Firstly, KRAS_SIGNALING_UP and KRAS_SIGNALING_DN gene sets, which represent genes upregulated and downregulated by KRAS respectively. Considering the observed lag in cell cycle progression by TLX^{+} cells, in combination with the well-established knowledge that KRAS regulates several proliferative signaling mechanisms, it is possible that the impact of TLX on cell cycle is at least in part mediated by its regulation of genes downstream of KRAS.

An additional gene set that TLX overexpression had a potent effect on was EPITHELIAL_MESENCHYMAL_TRANSITION (EMT) (Figure 3F). Intriguingly, EMT was repressed in siCon-TLX^{+} conditions, which was reversed under siTLX conditions (Fig. 3E–F). EMT is a hallmark for cancer cell invasion and metastasis [45]. These data suggest that enhanced expression of TLX in a TNBC cell line promotes a transcriptional program that likely impacts two crucial hallmarks of cancer: sustained proliferative signaling and activation of invasion and metastasis [46]. Overall, these results support an anti-oncogenic function for TLX in TNBC.

TLX impedes migration and invasion of MDA-MB-231 TNBC cells

Since genes associated with EMT were highlighted by GSEA (Fig. 3E–F), and EMT is known to promote the migratory and invasive properties of cancer cells, we next assessed the ability of TLX to modulate these aspects of cancer biology.

Using the classic “wound healing” scratch assay, we found that migration through time was reduced in TLX^{+} cells, with similar results being obtained in MDA-MB-231 and MDA- MB-468 cell models (Fig. 4A–B, Supplementary Fig. 6A). Migratory capacity is required for initial steps of metastasis, but invasive properties are required for invasion of peripheral tissue and intravasation into the blood stream. While migration and invasion are often correlated, they are distinct processes. Therefore, we performed invasion assays using transwell inserts coated with a commercial basement membrane. Similar to migratory

capacity, invasion through a basement membrane was decreased in TLX^+ cells (Fig. 4C–D). These findings were consistent for both MDA-MB-231 and MDA-MB-468 models (Fig. 4C–D, Supplementary Fig. 6B).

TLX impairs the growth of TNBC tumors in xenograft models and regulates pathways associated with progression

In order to evaluate the influence of TLX on tumor growth and metastasis, we first orthotopically grafted TLX^{con} or TLX^+ MDA-MB-231 cells into the axial mammary gland of athymic nude mice. Our primary endpoints were final tumor volume, final tumor weight at necropsy and time to reach 125, 200 and 315 mm^3, over a 53-day period. A single TLX^{con} mouse was euthanized 51 days post-graft due to unexpected weight loss. As can be seen in Fig 5A–C, TLX^{con} tumors grew significantly faster than TLX^+ tumors throughout the duration of the study, as well as having significantly larger final tumor volumes and weights. TLX^{con} tumors reached volumes of 125 mm^3, 200 mm^3 and 315 mm^3 sooner than TLX^+ tumors as assessed by Kaplan Meier (Gehan-Breslow-Wilcoxon test) analysis (Fig. 5D–F). Analysis by qPCR of tumors retrieved at necropsy indicated that TLX continued to be overexpressed in TLX^+ compared to TLX^{con} tumors (Fig 5G). This xenograft study was repeated independently at a different time, with similar results being obtained (Supplementary Fig. 7).

In order to gain more insight into the potential mechanisms by which TLX was mediating decreased tumor growth and metastatic colonization, as well as assess components of the microenvironment, we performed targeted transcriptome analysis on MDA-MB-231 tumors using NanoString technology (nCounter Breast Cancer 360 panel: https://www.nanostring.com/products/ncounter-assays-panels/oncology/breast-cancer-360/), which is curated for 776 different gene transcripts. 8 genes were found to be upregulated in TLX^+ tumors, while 18 genes were significantly downregulated (Fig. 5H–I). Downregulated genes (Fig. 5I) were then submitted to the online PANTHER Classification System (http://www.pantherdb.org/) which identifies pathways that are statistically overrepresented [43]. Interestingly, this analysis showed that several pathways that are known for their involvement in tumor progression, such as PI3 Kinase, EGFR and Angiogenesis were enriched for genes that were downregulated in TLX^+ xenograft tumors (Fig. 5I–J). These results demonstrate that TLX can regulate genes involved in oncogenic pathways in the *in vivo* setting and that there is a possible connection between the repression of these genes and the growth capacity of a TNBC tumor.

TLX Decreases Invasion and Metastatic Colonization *in vivo.*

Standard histopathologic analysis by a board-certified veterinary pathologist blinded to experimental design and treatment status revealed that MDA-MB-231 TLX^{con} and TLX^+ tumors had nearly an equal degree of tumoral necrosis (Fig. 6A). On the other hand, lymphatic invasion was documented in ~78% of control tumors compared to ~44% of TLX^+ tumors (Fig. 6B).

The observation of increased lymphatic invasion (Fig. 6B) was important given our findings that both migration and invasion were decreased in TLX^+ cells. This would suggest that

the metastatic colonization potential may be altered by TLX. To test this, we utilized a model where cells are grafted intravenously and must extravasate and invade at distal sites followed by colonization and outgrowth. 8 weeks following graft of MDA-MB-231 cells, lungs were visually assessed for macroscopic metastatic nodules. In support of our hypothesis that TLX alters metastatic invasion and colonization, lungs from mice that were grafted with TLX^+ cells had significantly fewer nodules compared to lungs from mice that received a graft of TLX^{con} cells (Fig. 6C). To evaluate this in greater detail and to capture micrometastases, lungs were sectioned, stained with H&E and assessed by a board-certified veterinary pathologist (blinded to experimental details). Significantly less lung involvement was observed in the lungs from mice grafted with TLX^+ cells (Fig. 6D). Finally, in order to quantify total metastatic burden, total RNA was extracted from one side of the lungs and qPCR analysis was performed for the NeoR gene, which is encoded by the vector in both TLX^+ and TLX^{con} cells. NeoR, and thus total metastatic burden, was significantly lower in the lungs of mice grafted with MDA-MB-231 TLX^+ cells compared to TLX^{con} (Fig. 6E) Importantly, these findings were recapitulated in mice grafted with MDA-MB-468 cells, where lungs from TLX^+ mice had significantly reduced total metastatic tumor burden as assessed by bioluminescence (Fig. 6F). Cumulatively, these results strongly support the notion that chronic elevation of TLX results in decreased EMT, and thus decreased capacity to migrate, invade and colonize distal tissues.

TLX upregulated gene signature is positively correlated with ER-negative survival

The combination of our clinical, transcriptomic, and *in vitro* and *in vivo* functional characterization assays strongly support the notion that TLX transcriptional regulation in TNBC can deter cancer progression. In order to determine which regulatory targets are likely contributing to the cancer-inhibitory effects of TLX, we used the data from RNA-Seq analysis (Fig. 3) combined with the available patient data from the METABRIC dataset. An iterative process (detailed in methods) which utilized features such as significance of expression change, fold-change in expression, and directionality of expression changes (i.e., negative or positive) resulted in a list of 117 downregulated genes and 11 upregulated genes (Supplemental Tables 3 and 4). Patients were parsed into high (top 25%) and low (bottom 25%) cohorts for the downregulated and upregulated signatures and then survival of those cohorts was assessed. For this analysis, each gene in the signature was weighted equally, despite the different fold changes observed in our RNA-seq analysis. TLX biology is generally considered to be transcriptionally repressive in nature which is evidenced by the more than 10-fold disparity between our downregulated and upregulated signature genes. Therefore, it was somewhat surprising that the 11 upregulated gene signature was correlated with improved RFS and OS in ERα-negative patients, whereas no survival correlation was found for our downregulated signature (Fig. 7A–D). Although not reaching statistical significance, likely due to the considerably smaller patient sample size, similar associations were observed in the basal-like patient population (Fig. 7E–H). The association of this signature continued to be evident when TLX was not included in the analysis (Supplemental Fig. 8). Therefore, unlike in cancers of the brain and prostate where TLX's well-known ability to inhibit tumor suppressors ultimately facilitates malignant progression, these data would suggest that TLX's pro-survival function in ERα-negative breast cancer patients is likely dependent on the upregulation of several key target genes

TLX regulation of SERPINB2 contributes to anti-migratory phenotype

Of the 11 genes from our upregulated gene signature (Figs. 3&7), serpin family B member 2 (*SERPINB2/PAI2*) was the most robustly upregulated (Supplemental Table 3). When SERPINB2 was not included in the signature, significance was lost, although the analysis was likely underpowered to draw firm conclusions (Supplemental Fig. 8). Intriguingly, previous work has demonstrated that SERPINB2 can impair cancer cell migration, invasion and metastasis [47–50]. Therefore, we chose to investigate if this gene was contributing to the observed migratory phenotype in our TLX^+ cells.

In agreement with our RNA-Seq results (Fig 3) qPCR analysis confirmed that SERPINB2 expression was heightened in our MDA-MB-231 TLX^+ cells compared to TLX^{con} cells, as well as in a second clone (clone 2) (Fig. 8A and Supplemental Fig. 9A). Additionally, TLX-specific regulation of SERPINB2 expression was demonstrated, as treatment of TLX^+ cells with siTLX reversed SERPINB2 expression back to control levels (Fig. 8A). This was confirmed in an independent experiment using a second targeting siRNA against TLX (Supplemental Fig. 9B–C). In order to directly test the impact of SERPINB2 on migration, we first validated the efficacy of an siRNA against SERPINB2 (siSERPINB2) in our MDA-MB-231 model using the following treatment groups: siCont-TLX^{con}, siCont-TLX^+ and siSERPINB2-TLX^+ (Fig. 8B). Similar to Fig. 4, we conducted migration assays, the results of which indicating that SERPINB2 was required for the anti-migratory effects of TLX. Specifically, siRNA knockdown of SERPINB2 increased gap closure through time and migratory velocity (Fig. 8C&D) in TLX^+ cells compared to siCont-TLX^+ cells, partially rescuing the effects of TLX overexpression (Fig. 8C). Taken together, these data suggest that SERPINB2 is a novel regulatory target of TLX, and that TLX's anti-migratory effects are at least in part mediated through this regulatory axis.

Discussion:

The paucity of clinically approved targeted therapeutics for the treatment of TNBC persists as a hindrance to our ability to improve the prognostic outlook for patients suffering from this aggressive breast cancer subtype. Although the immune system holds much promise [51], combination of immune checkpoint inhibitors with chemotherapeutic agents is only approved for a subpopulation of TNBC patients, and even then, has limited efficacy [52, 53]. Therefore, alternative therapies are still required for the treatment of TNBC.

Since nuclear receptors are highly amenable to small molecule intervention, we utilized tumoral gene expression and patient survival data to identify nuclear receptors that may influence the pathophysiology of TNBC. TLX emerged as a strong candidate as (1) it had elevated expression in patients with ERα-negative breast cancers, and (2) higher expression of TLX was correlated with improved survival.

Using two different TNBC cell lines, we first demonstrated that stable overexpression of TLX alone could impair *in vitro* proliferation, and subsequent primary tumor growth in a murine model. This is in contrast to reports from neural progenitor cells and other cancer types, where TLX generally promotes proliferation [19, 20, 23–30, 54]. Even previous work with MDA-MB-231 cells indicated that TLX was pro-proliferative [30]. At this point,

the reasons for these discrepancies are not clear, although it is possible that (1) TLX has cancer-type specific roles, and/or (2) chronic perturbances in TLX result in different biological effects than acute manipulation. However, for TNBC, it is also likely that short term perturbations in TLX result in different phenotypes than prolonged changes, as we have demonstrated for proliferation (Fig. 2).

RNA-Seq analysis demonstrated that chronic overexpression of TLX resulted in the downregulation of numerous genes implicated in the pro-proliferative KRAS signaling. In other experiments, we found that cell cycle progression was altered, but not apoptosis, DNA synthesis or senescence. Thus, the observed decreased proliferation was likely due to altered KRAS signaling and cell cycle progression. Interestingly, the RNA-Seq analysis also revealed EMT as being altered, a process well-known for its roles in migration, invasion and metastasis [55], with the assumption that the single TLX^+ clone used for this analysis is reflective of generalized TLX overexpression. It was also interesting that of the 5,967 genes differentially expressed in TLX^+ compared to TLX^{con} cells, siRNA only recovered 1,326 genes. We propose two potential reasons for this: (1) Kinetics. The siRNA treatment was only for 48hrs while the overexpression was stable for several passages. It is possible that the acute knockdown did not provide sufficient time for the effects of secondary targets (such as transcription factors etc.) to be observed. (2) Altered epigenome. Since these cells were chronically overexpressing TLX it is possible that the epigenome was altered in a way that simply removing TLX would not result in altered gene expression. Either way, future studies should be performed to elucidate this biology.

Upon further experimentation, we found that indeed, TLX significantly impeded both cell migration and cell invasion in TNBC. The pathological relevance of these findings is demonstrated by decreased lymphatic involvement of primary tumors and decreased metastatic colonization in murine models (Fig. 6). These findings are in agreement with previous work indicating that TLX overexpression in glioma stem cells or treatment of glioblastoma cells with propranolol (a purported TLX agonist), impedes migration [56, 57]. However, other reports in TNBC and neuroblastoma contrast these findings, where TLX promoted migration and invasion, potentially through the regulation of matrix metalloproteinases and other EMT-related genes [26, 30]. Therefore, it is concluded that the role of TLX in cancer is complex, exerting differential effects depending on (1) the temporal nature of its overexpression or activity, and (2) cancer cell context. Furthermore, analyses of other unique TNBC models will be required to capture the complex heterogeneity of human disease.

While the inhibition of genes in the pathways identified in our GSEA analysis likely represent important targets mediating the observed effects of TLX overexpression, one of the more surprising results of our work was that the TLX upregulated gene signature, rather than the downregulated gene signature, was correlated with improved recurrent-free and overall survival in ERα-negative patients, with highly similar results being observed in basal-like patients too. These results not only indicate that TLX's anti-cancer effects are likely the result of a dynamic mixture of downregulating and upregulating target genes, but the importance of evaluating both the predominant (transcriptional repression) and less frequently observed (transcriptional activation) functions of cancer regulatory molecules.

It was of interest that SERPINB2 was very robustly upregulated by TLX as identified in our RNA-seq analysis of MDA-MB-231 cells. Important future work will be aimed at determining the mechanisms by which TLX regulates SERPINB2. SERPINB2, along with its closely related family member, SERPINE1, both function as inhibitors of urokinase plasminogen activator (*uPA*). However, due to structural differences, these two proteins appear to have opposing roles when it comes to cancer, with SERPINE1 promoting proliferation and migration, and SERPINB2 opposing these functions [58]. Importantly, we found that SERPINB2 was required for the full inhibitory effects of TLX on migration. Thus, it is likely that at least some of the modulatory activities TLX has on migration are due to its induction of SERPINB2.

Collectively, our results demonstrate that cancer cell-intrinsic expression of TLX inhibits two hallmarks of cancer, proliferation and invasion, resulting in impaired tumor growth and metastasis. Taking into consideration the described impact of TLX in other cancers, it is likely that the role of TLX is highly context-dependent. Determining conditions where TLX is inhibitory will be important for the future development of TLX as a therapeutic target. Recently published work that has potentially "de-orphanized" TLX presented evidence that oleic acid is a bonafide endogenous ligand for this receptor, a finding that provides critical insight into TLX physiology and future targeted drug development [59]. It will be important to utilize the *in vitro* models described in this paper to evaluate the effects, if any, of oleic acid, and ascribe those to TLX. Furthermore, it is important to consider that we have only explored the roles of TLX within the TNBC cells themselves, and the functional importance of TLX within stromal cells remains to be determined; many nuclear receptors being reported to have roles in immune cells [17]. This will be an important consideration given the recent breakthroughs of immune-based therapies. In summary, TLX may represent a new therapeutic target for the treatment of TNBC, but more work is required to evaluate the precise context-dependent roles of this receptor.

Supplementary Material

Refer to Web version on PubMed Central for supplementary material.

Acknowledgments

This work was supported by grants from the following sources: National Cancer Institute of the National Institutes of Health (R01CA234025 to ERN, R01CA211875 to MJS, and CA260819 to DAG). Department of Defense Breast Cancer Research Program Era of Hope Scholar Award (W81XWH-20-BCRP-EOHS / BC200206 to ERN). Department of Defense Prostate Cancer Research Program Impact Award (W81XWH2110903 to MJS). American Institute for Cancer Research (713063 to ERN). LM was supported by a Julie and David Mead Endowed Graduate Student Fellowship. HEVG was supported by the NIH Chemistry-Biology Interface Training Grant (T32-GM136629). ATN was supported by the NIH Research Training Program in Toxicology and Environmental Health (T32 ES007326). MTM was the recipient of a University of Illinois School of Molecular and Cellular Biology Summer Undergraduate Research Fellowship.

References Cited

[1]. Borri F, Granaglia A, Pathology of triple negative breast cancer, Seminars in Cancer Biology, 72 (2021) 136–145. [PubMed: 32544511]

[2]. Wahba HA, El-Hadaad HA, Current approaches in treatment of triple-negative breast cancer, Cancer Biol Med, 12 (2015) 106–116. [PubMed: 26175926]

[3]. Berry DA, Cirrincione C, Henderson IC, Citron ML, Budman DR, Goldstein LJ, Martino S, Perez EA, Muss HB, Norton L, Hudis C, Winer EP, Estrogen-receptor status and outcomes of modern chemotherapy for patients with node-positive breast cancer, Jama, 295 (2006) 1658–1667. [PubMed: 16609087]

[4]. van der Hage JA, Mieog JS, van de Vijver MJ, van de Velde CJ, Efficacy of adjuvant chemotherapy according to hormone receptor status in young patients with breast cancer: a pooled analysis, Breast Cancer Res, 9 (2007) R70. [PubMed: 17931406]

[5]. Hall E, Cameron D, Waters R, Barrett-Lee P, Ellis P, Russell S, Bliss JM, Hopwood P, Comparison of patient reported quality of life and impact of treatment side effects experienced with a taxane-containing regimen and standard anthracycline based chemotherapy for early breast cancer: 6 year results from the UK TACT trial (CRUK/01/001), Eur J Cancer, 50 (2014) 2375–2389. [PubMed: 25065293]

[6]. Zheng R, Han S, Duan C, Chen K, You Z, Jia J, Lin S, Liang L, Liu A, Long H, Wang S, Role of taxane and anthracycline combination regimens in the management of advanced breast cancer: a meta-analysis of randomized trials, Medicine (Baltimore), 94 (2015) e803. [PubMed: 25929935]

[7]. Wu X, Baig A, Kasymjanova G, Kafi K, Holcroft C, Mekouar H, Carbonneau A, Bahoric B, Sultanem K, Muanza T, Pattern of Local Recurrence and Distant Metastasis in Breast Cancer By Molecular Subtype, Cureus, 8 (2016) e924. [PubMed: 28090417]

[8]. Anders C, Carey LA, Understanding and treating triple-negative breast cancer, Oncology (Williston Park), 22 (2008) 1233–1239; discussion 1239–1240, 1243. [PubMed: 18980022]

[9]. Adams S, Schmid P, Rugo HS, Winer EP, Loirat D, Awada A, Cescon DW, Iwata H, Campone M, Nanda R, Hui R, Curigliano G, Toppmeyer D, O'Shaughnessy J, Loi S, Paluch-Shimon S, Tan AR, Card D, Zhao J, Karantza V, Cortés J, Pembrolizumab monotherapy for previously treated metastatic triple-negative breast cancer: cohort A of the phase II KEYNOTE-086 study, Ann Oncol, 30 (2019) 397–404. [PubMed: 30475950]

[10]. Bardia A, Mayer IA, Vahdat LT, Tolaney SM, Isakoff SJ, Diamond JR, O'Shaughnessy J, Moroose RL, Santin AD, Abramson VG, Shah NC, Rugo HS, Goldenberg DM, Sweidan AM, Iannone R, Washkowitz S, Sharkey RM, Wegener WA, Kalinsky K, Sacituzumab Govitecan-hziy in Refractory Metastatic Triple-Negative Breast Cancer, New England Journal of Medicine, 380 (2019) 741–751. [PubMed: 30786188]

[11]. Kim SB, Dent R, Im SA, Espié M, Blau S, Tan AR, Isakoff SJ, Oliveira M, Saura C, Wongchenko MJ, Kapp AV, Chan WY, Singel SM, Maslyar DJ, Baselga J, Ipatasertib plus paclitaxel versus placebo plus paclitaxel as first-line therapy for metastatic triple-negative breast cancer (LOTUS): a multicentre, randomised, double-blind, placebo-controlled, phase 2 trial, Lancet Oncol, 18 (2017) 1360–1372. [PubMed: 28800861]

[12]. Schmid P, Adams S, Rugo HS, Schneeweiss A, Barrios CH, Iwata H, Diéras V, Hegg R, Im S-A, Shaw Wright G, Henschel V, Molinero L, Chui SY, Funke R, Husain A, Winer EP, Loi S, Emens LA, Atezolizumab and Nab-Paclitaxel in Advanced Triple-Negative Breast Cancer, New England Journal of Medicine, 379 (2018) 2108–2121. [PubMed: 30345906]

[13]. Robson M, Im SA, Senkus E, Xu B, Domchek SM, Masuda N, Delaloge S, Li W, Tung N, Armstrong A, Wu W, Goessl C, Runswick S, Conte P, Olaparib for Metastatic Breast Cancer in Patients with a Germline BRCA Mutation, N Engl J Med, 377 (2017) 523–533. [PubMed: 28578601]

[14]. Polk A, Svane IM, Andersson M, Nielsen D, Checkpoint inhibitors in breast cancer - Current status, Cancer Treat Rev, 63 (2018) 122–134. [PubMed: 29287242]

[15]. Swoboda A, Nanda R, Immune Checkpoint Blockade for Breast Cancer, Cancer Treat Res, 173 (2018) 155–165. [PubMed: 29349763]

[16]. Mangelsdorf DJ, Thummel C, Beato M, Herrlich P, Schütz G, Umesono K, Blumberg B, Kastner P, Mark M, Chambon P, Evans RM, The nuclear receptor superfamily: the second decade, Cell, 83 (1995) 835–839. [PubMed: 8521507]

[17]. Shahoei SH, Nelson ER, Nuclear receptors, cholesterol homeostasis and the immune system, The Journal of steroid biochemistry and molecular biology, 191 (2019) 105364. [PubMed: 31002862]

[18]. Muscat GE, Eriksson NA, Byth K, Loi S, Graham D, Jindal S, Davis MJ, Clyne C, Funder JW, Simpson ER, Ragan MA, Kuczek E, Fuller PJ, Tilley WD, Leedman PJ, Clarke CL, Research

resource: nuclear receptors as transcriptome: discriminant and prognostic value in breast cancer, Mol Endocrinol, 27 (2013) 350–365. [PubMed: 23292282]

[19]. Zhang CL, Zou Y, Yu RT, Gage FH, Evans RM, Nuclear receptor TLX prevents retinal dystrophy and recruits the corepressor atrophin1, Genes Dev, 20 (2006) 1308–1320. [PubMed: 16702404]

[20]. Sun G, Yu RT, Evans RM, Shi Y, Orphan nuclear receptor TLX recruits histone deacetylases to repress transcription and regulate neural stem cell proliferation, Proc Natl Acad Sci U S A, 104 (2007) 15282–15287. [PubMed: 17873065]

[21]. Monaghan AP, Bock D, Gass P, Schwäger A, Wolfer DP, Lipp HP, Schütz G, Defective limbic system in mice lacking the tailless gene, Nature, 390 (1997) 515–517. [PubMed: 9394001]

[22]. Roy K, Thiels E, Monaghan AP, Loss of the tailless gene affects forebrain development and emotional behavior, Physiol Behav, 77 (2002) 595–600. [PubMed: 12527005]

[23]. Shi Y, Chichung Lie D, Taupin P, Nakashima K, Ray J, Yu RT, Gage FH, Evans RM, Expression and function of orphan nuclear receptor TLX in adult neural stem cells, Nature, 427 (2004) 78–83. [PubMed: 14702088]

[24]. Liu HK, Wang Y, Belz T, Bock D, Takacs A, Radlwimmer B, Barbus S, Reifenberger G, Lichter P, Schütz G, The nuclear receptor tailless induces long-term neural stem cell expansion and brain tumor initiation, Genes Dev, 24 (2010) 683–695. [PubMed: 20360385]

[25]. Zou Y, Niu W, Qin S, Downes M, Burns DK, Zhang CL, The nuclear receptor TLX is required for gliomagenesis within the adult neurogenic niche, Mol Cell Biol, 32 (2012) 4811–4820. [PubMed: 23028043]

[26]. Chavali PL, Saini RK, Zhai Q, Vizlin-Hodzic D, Venkatabalasubramanian S, Hayashi A, Johansson E, Zeng ZJ, Mohlin S, Påhlman S, Hansford L, Kaplan DR, Funa K, TLX activates MMP-2, promotes self-renewal of tumor spheres in neuroblastoma and correlates with poor patient survival, Cell Death Dis, 5 (2014) e1502. [PubMed: 25356871]

[27]. Cui Q, Yang S, Ye P, Tian E, Sun G, Zhou J, Sun G, Liu X, Chen C, Murai K, Zhao C, Azizian KT, Yang L, Warden C, Wu X, D'Apuzzo M, Brown C, Badie B, Peng L, Riggs AD, Rossi JJ, Shi Y, Downregulation of TLX induces TET3 expression and inhibits glioblastoma stem cell self-renewal and tumorigenesis, Nat Commun, 7 (2016) 10637. [PubMed: 26838672]

[28]. Wu D, Yu S, Jia L, Zou C, Xu Z, Xiao L, Wong KB, Ng CF, Chan FL, Orphan nuclear receptor TLX functions as a potent suppressor of oncogene-induced senescence in prostate cancer via its transcriptional co-regulation of the CDKN1A (p21(WAF1) (/) (CIP1)) and SIRT1 genes, J Pathol, 236 (2015) 103–115. [PubMed: 25557355]

[29]. Jia L, Wu D, Wang Y, You W, Wang Z, Xiao L, Cai G, Xu Z, Zou C, Wang F, Teoh JY-C, Ng C-F, Yu S, Chan FL, Orphan nuclear receptor TLX contributes to androgen insensitivity in castration-resistant prostate cancer via its repression of androgen receptor transcription, Oncogene, 37 (2018) 3340–3355. [PubMed: 29555975]

[30]. Lin ML, Patel H, Remenyi J, Banerji CR, Lai CF, Periyasamy M, Lombardo Y, Busonero C, Ottaviani S, Passey A, Quinlan PR, Purdie CA, Jordan LB, Thompson AM, Finn RS, Rueda OM, Caldas C, Gil J, Coombes RC, Fuller-Pace FV, Teschendorff AE, Buluwela L, Ali S, Expression profiling of nuclear receptors in breast cancer identifies TLX as a mediator of growth and invasion in triple-negative breast cancer, Oncotarget, 6 (2015) 21685–21703. [PubMed: 26280373]

[31]. Győrffy B, Survival analysis across the entire transcriptome identifies biomarkers with the highest prognostic power in breast cancer, Comput Struct Biotechnol J, 19 (2021) 4101–4109. [PubMed: 34527184]

[32]. Cerami E, Gao J, Dogrusoz U, Gross BE, Sumer SO, Aksoy BA, Jacobsen A, Byrne CJ, Heuer ML, Larsson E, Antipin Y, Reva B, Goldberg AP, Sander C, Schultz N, The cBio cancer genomics portal: an open platform for exploring multidimensional cancer genomics data, Cancer Discov, 2 (2012) 401–404. [PubMed: 22588877]

[33]. Gao J, Aksoy BA, Dogrusoz U, Dresdner G, Gross B, Sumer SO, Sun Y, Jacobsen A, Sinha R, Larsson E, Cerami E, Sander C, Schultz N, Integrative analysis of complex cancer genomics and clinical profiles using the cBioPortal, Sci Signal, 6 (2013) pl1. [PubMed: 23550210]

[34]. Curtis C, Shah SP, Chin S-F, Turashvili G, Rueda OM, Dunning MJ, Speed D, Lynch AG, Samarajiwa S, Yuan Y, Gräf S, Ha G, Haffari G, Bashashati A, Russell R, McKinney S, Caldas

C, Aparicio S, Curtis† C, Shah SP, Caldas C, Aparicio S, Brenton JD, Ellis I, Huntsman D, Pinder S, Purushotham A, Murphy L, Caldas C, Aparicio S, Caldas C, Bardwell H, Chin S-F, Curtis C, Ding Z, Gräf S, Jones L, Liu B, Lynch AG, Papatheodorou I, Sammut SJ, Wishart G, Aparicio S, Chia S, Gelmon K, Huntsman D, McKinney S, Speers C, Turashvili G, Watson P, Ellis I, Blamey R, Green A, Macmillan D, Rakha E, Purushotham A, Gillett C, Grigoriadis A, Pinder S, de Rinaldis E, Tutt A, Murphy L, Parisien M, Troup S, Caldas C, Chin S-F, Chan D, Fielding C, Maia A-T, McGuire S, Osborne M, Sayalero SM, Spiteri I, Hadfield J, Aparicio S, Turashvili G, Bell L, Chow K, Gale N, Huntsman D, Kovalik M, Ng Y, Prentice L, Caldas C, Tavaré S, Curtis C, Dunning MJ, Gräf S, Lynch AG, Rueda OM, Russell R, Samarajiwa S, Speed D, Markowetz F, Yuan Y, Brenton JD, Aparicio S, Shah SP, Bashashati A, Ha G, Haffari G, McKinney S, Langerød A, Green A, Provenzano E, Wishart G, Pinder S, Watson P, Markowetz F, Murphy L, Ellis I, Purushotham A, Børresen-Dale A-L, Brenton JD, Tavaré S, Caldas C, Aparicio S, Group M, Co c., Writing c., Steering c., Tissue s. clinical data source, U.K.C.R.I. University of Cambridge/Cancer Research, A. British Columbia Cancer, N. University of, L. King's College, B. Manitoba Institute of Cell, c. Cancer genome/transcriptome characterization, s. Data analysis, The genomic and transcriptomic architecture of 2,000 breast tumours reveals novel subgroups, Nature, 486 (2012) 346–352. [PubMed: 22522925]

[35]. Lanczky A, Gyorffy B, Web-Based Survival Analysis Tool Tailored for Medical Research (KMplot): Development and Implementation, J Med Internet Res, 23 (2021) e27633. [PubMed: 34309564]

[36]. Nelson ER, DuSell CD, Wang X, Howe MK, Evans G, Michalek RD, Umetani M, Rathmell JC, Khosla S, Gesty-Palmer D, McDonnell DP, The oxysterol, 27-hydroxycholesterol, links cholesterol metabolism to bone homeostasis through its actions on the estrogen and liver X receptors, Endocrinology, 152 (2011) 4691–4705. [PubMed: 21933863]

[37]. Javanmoghadam-Kamrani S, Keyomarsi K, Synchronization of the cell cycle using lovastatin, Cell Cycle, 7 (2008) 2434–2440. [PubMed: 18677105]

[38]. Schneider CA, Rasband WS, Eliceiri KW, NIH Image to ImageJ: 25 years of image analysis, Nature Methods, 9 (2012) 671–675. [PubMed: 22930834]

[39]. Suarez-Arnedo A, Torres Figueroa F, Clavijo C, Arbeláez P, Cruz JC, Muñoz-Camargo C, An image J plugin for the high throughput image analysis of in vitro scratch wound healing assays, PLoS One, 15 (2020) e0232565. [PubMed: 32722676]

[40]. He S, Ma L, Baek AE, Vardanyan A, Vembar V, Chen JJ, Nelson AT, Burdette JE, Nelson ER, Host CYP27A1 expression is essential for ovarian cancer progression, Endocr Relat Cancer, 26 (2019) 659–675. [PubMed: 31048561]

[41]. Liberzon A, Birger C, Thorvaldsdóttir H, Ghandi M, Mesirov JP, Tamayo P, The Molecular Signatures Database (MSigDB) hallmark gene set collection, Cell Syst, 1 (2015) 417–425. [PubMed: 26771021]

[42]. Geiss GK, Bumgarner RE, Birditt B, Dahl T, Dowidar N, Dunaway DL, Fell HP, Ferree S, George RD, Grogan T, James JJ, Maysuria M, Mitton JD, Oliveri P, Osborn JL, Peng T, Ratcliffe AL, Webster PJ, Davidson EH, Hood L, Dimitrov K, Direct multiplexed measurement of gene expression with color-coded probe pairs, Nature Biotechnology, 26 (2008) 317–325.

[43]. Mi H, Ebert D, Muruganujan A, Mills C, Albou L-P, Mushayamaha T, Thomas PD, PANTHER version 16: a revised family classification, tree-based classification tool, enhancer regions and extensive API, Nucleic Acids Research, 49 (2020) D394–D403.

[44]. Nelson AT, Wang Y, Nelson ER, TLX, an Orphan Nuclear Receptor With Emerging Roles in Physiology and Disease, Endocrinology, 162 (2021).

[45]. Zhang Y, Weinberg RA, Epithelial-to-mesenchymal transition in cancer: complexity and opportunities, Front Med, 12 (2018) 361–373. [PubMed: 30043221]

[46]. Hanahan D, Weinberg RA, The hallmarks of cancer, Cell, 100 (2000) 57–70. [PubMed: 10647931]

[47]. Laug WE, Cao XR, Yu YB, Shimada H, Kruithof EK, Inhibition of invasion of HT1080 sarcoma cells expressing recombinant plasminogen activator inhibitor 2, Cancer Res, 53 (1993) 6051–6057. [PubMed: 8261421]

[48]. Zhang XM, Wang T, Hu P, Li B, Liu H, Cheng YF, SERPINB2 overexpression inhibited cell proliferation, invasion and migration, led to G2/M arrest, and increased radiosensitivity in nasopharyngeal carcinoma cells, J Radiat Res, 60 (2019) 318–327. [PubMed: 30864656]

[49]. Mueller BM, Yu YB, Laug WE, Overexpression of plasminogen activator inhibitor 2 in human melanoma cells inhibits spontaneous metastasis in scid/scid mice, Proceedings of the National Academy of Sciences, 92 (1995) 205–209.

[50]. Praus M, Wauterickx K, Collen D, Gerard RD, Reduction of tumor cell migration and metastasis by adenoviral gene transfer of plasminogen activator inhibitors, Gene Therapy, 6 (1999) 227–236. [PubMed: 10435107]

[51]. Bianchini G, De Angelis C, Licata L, Gianni L, Treatment landscape of triple-negative breast cancer — expanded options, evolving needs, Nature Reviews Clinical Oncology, (2021).

[52]. Thomas R, Al-Khadairi G, Decock J, Immune Checkpoint Inhibitors in Triple Negative Breast Cancer Treatment: Promising Future Prospects, Frontiers in oncology, 10 (2020) 600573. [PubMed: 33718107]

[53]. Schmid P, Rugo HS, Adams S, Schneeweiss A, Barrios CH, Iwata H, Dieras V, Henschel V, Molinero L, Chui SY, Maiya V, Husain A, Winer EP, Loi S, Emens LA, Investigators IM, Atezolizumab plus nab-paclitaxel as first-line treatment for unresectable, locally advanced or metastatic triple-negative breast cancer (IMpassion130): updated efficacy results from a randomised, double-blind, placebo-controlled, phase 3 trial, Lancet Oncol, 21 (2020) 44–59. [PubMed: 31786121]

[54]. Li W, Sun G, Yang S, Qu Q, Nakashima K, Shi Y, Nuclear receptor TLX regulates cell cycle progression in neural stem cells of the developing brain, Mol Endocrinol, 22 (2008) 56–64. [PubMed: 17901127]

[55]. Lambert AW, Pattabiraman DR, Weinberg RA, Emerging Biological Principles of Metastasis, Cell, 168 (2017) 670–691. [PubMed: 28187288]

[56]. Li GL, Fang SH, Xu B, Monitoring in real time the effect of TLX overexpression on proliferation and migration of C6 cells, Neoplasma, 64 (2017) 48–55. [PubMed: 27881004]

[57]. Faudone G, Bischoff-Kont I, Rachor L, Willems S, Zhubi R, Kaiser A, Chaikuad A, Knapp S, Fürst R, Heering J, Merk D, Propranolol Activates the Orphan Nuclear Receptor TLX to Counteract Proliferation and Migration of Glioblastoma Cells, J Med Chem, 64 (2021) 8727–8738. [PubMed: 34115934]

[58]. Croucher DR, Saunders DN, Lobov S, Ranson M, Revisiting the biological roles of PAI2 (SERPINB2) in cancer, Nature Reviews Cancer, 8 (2008) 535–545. [PubMed: 18548086]

[59]. Kandel P, Semerci F, Mishra R, Choi W, Bajic A, Baluya D, Ma L, Chen K, Cao AC, Phongmekhin T, Matinyan N, Jiménez-Panizo A, Chamakuri S, Raji IO, Chang L, Fuentes-Prior P, MacKenzie KR, Benn CL, Estébanez-Perpiñá E, Venken K, Moore DD, Young DW, Maletic-Savatic M, Oleic acid is an endogenous ligand of TLX/NR2E1 that triggers hippocampal neurogenesis, Proc Natl Acad Sci U S A, 119 (2022) e2023784119. [PubMed: 35333654]

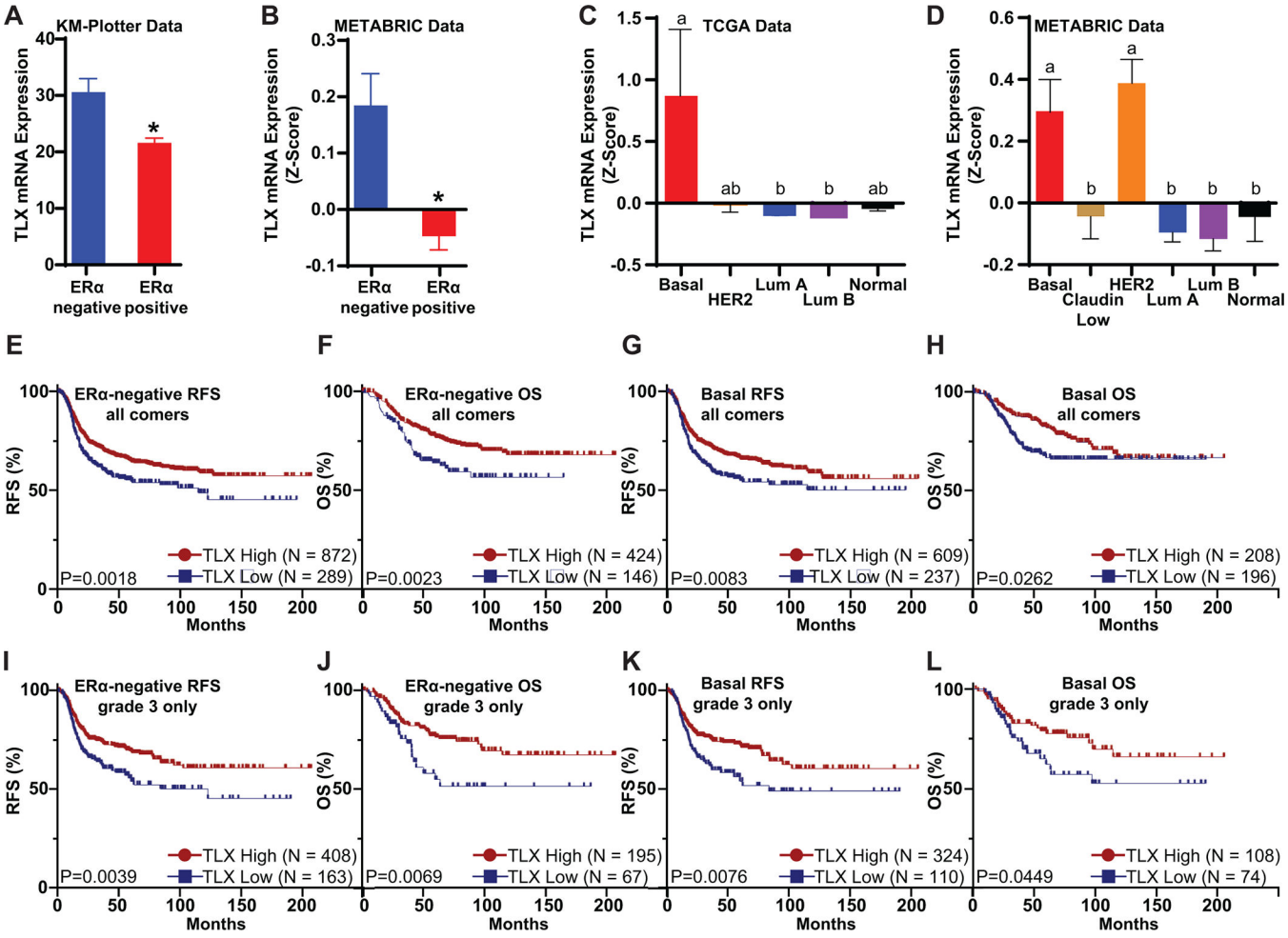

Figure 1. TLX Expression is elevated in ERα-negative and basal breast tumors and is positively correlated with survival.

A & B TLX mRNA expression is higher in ERα-negative compared to ERα-positive tumors, as evaluated in the (**A**) KM Plotter (relative expression) and (**B**) METABRIC data sets (N = 4929 & N = 1904 respectively). Data are expressed as mean ±SEM An asterisk (*) indicates statistical significance ($p < 0.05$, student's unpaired two-tailed t test). **C & D** TLX mRNA expression is higher in the Basal PAM50 subtype compared to other subtypes, as assessed in the (**C**) TCGA and (**D**) METABRIC data sets (N = 981 & N = 1898 respectively). Data are expressed as mean ±SEM. Different letters denote statistical significance ($p < 0.05$, one-way ANOVA followed by Tukey's multiple comparisons test). **E-L** Higher TLX mRNA expression in the KM Plotter data sets is correlated with longer recurrence-free survival (RFS) and overall survival (OS) in both ERα-negative and basal-like patients. Kaplan-Meier analysis followed by the log-rank test (p-value indicated on graph) was performed. High and low expression of TLX was established using the most significant cut off per query. [E: high N=872, low N=289, F: high N=424, low N=146, G: high N=609, low N=237, H: High N=208, Low N=196, I: High N=408, Low N=163, J: High N=195, Low N=67, K: High N=324, Low N=110, L: High N=108, Low N=74].

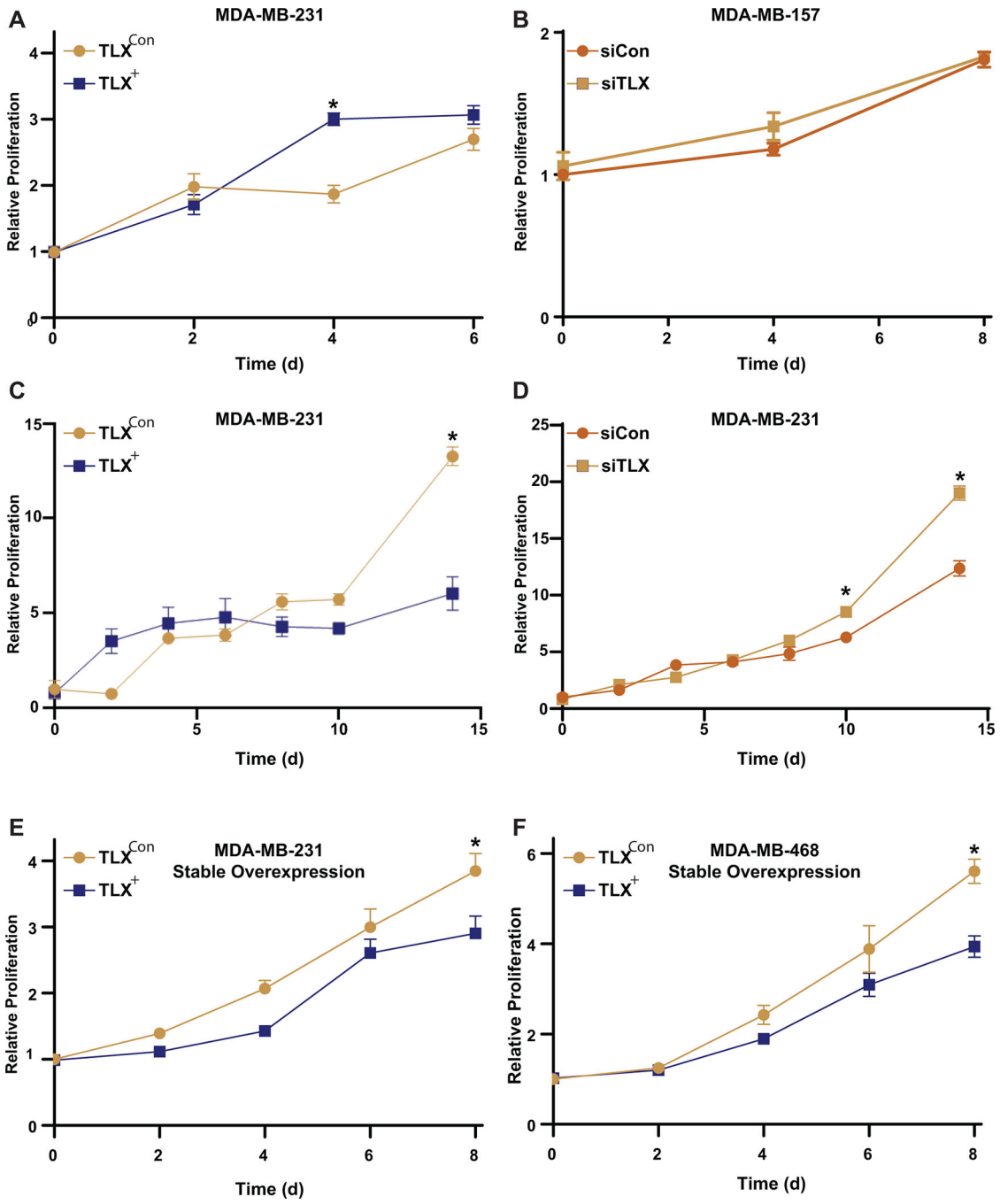

Figure 2. Chronic overexpression of TLX reduces proliferation of cellular models of TNBC.

A Short-term transient overexpression of TLX in the TNBC cell line MDA-MB-231 temporarily increased proliferation (N = 12 internal replicates/condition). **B** Short-term transient knockdown of TLX in the TNBC cell line MDA-MB-157 had no effect on proliferation (N = 6 internal replicates/condition, showing one representative experiment of three experiments, additional TLX targeting siRNA shown in Supplemental Fig. 2D). **C & D** Extended assays (14 d) using transient overexpression or knockdown of TLX in MDA-MB-231 cells either inhibited or promoted proliferation, respectively (N = 4

internal replicates/condition, showing one representative experiment of three), additional TLX targeting siRNA shown in Supplemental Fig. 2E). **E & F** Stable overexpression of TLX in MDA-MB-231 and MDA-MB-468 cells (another TNBC cell line) inhibited proliferation (N = 6 internal replicates/condition, showing one representative experiment of three). Data are expressed as mean ±SEM. An asterisk (*) indicates statistical significance at that timepoint ($p < 0.05$, two-way ANOVA followed by Sidak's multiple comparison test).

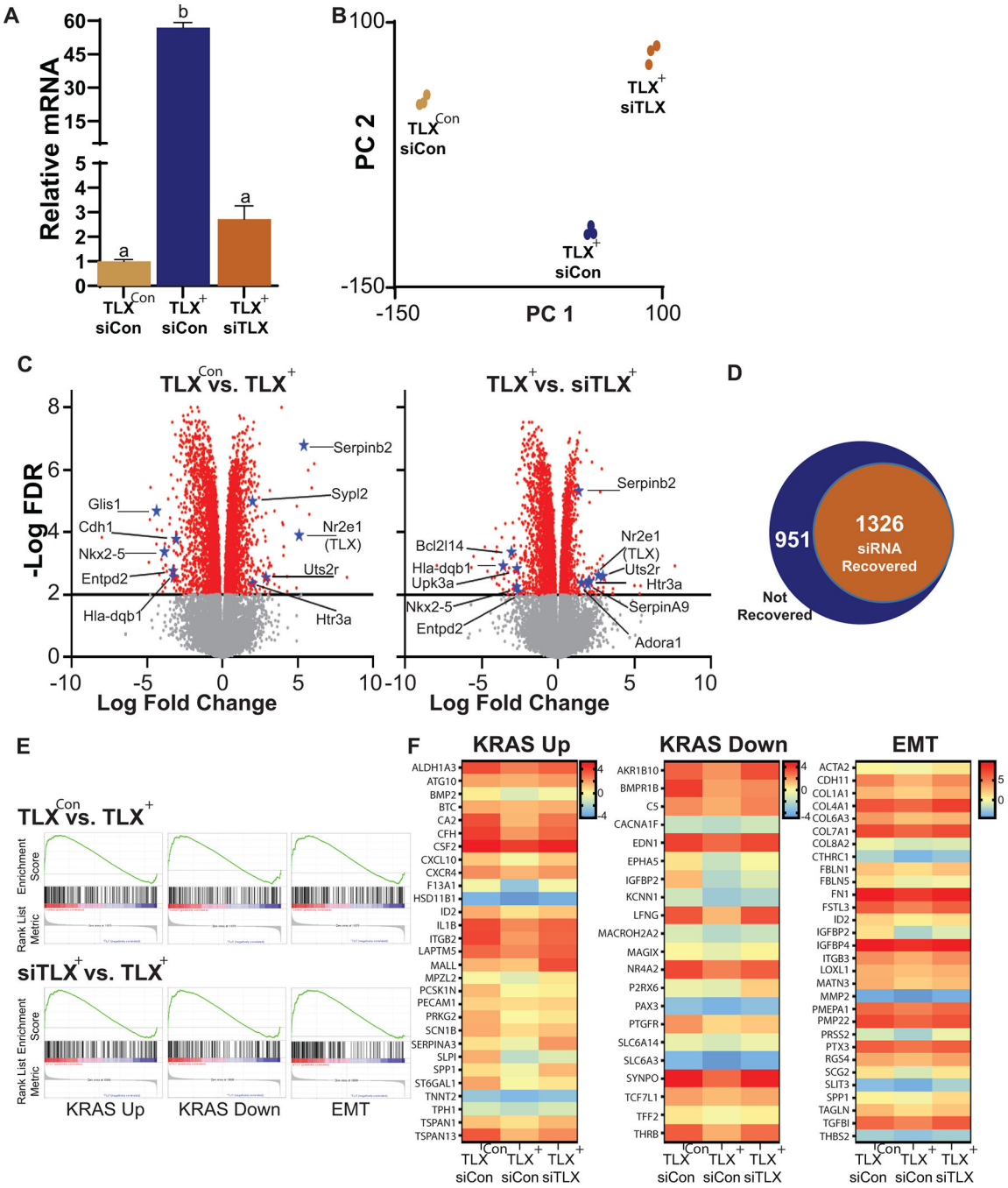

Figure 3. Stable overexpression of TLX results in a unique transcriptional profile in MDA-MB-231 cells.

MDA-MB-231 cells stably expressing a control empty vector (single cell clone, TLX^{con}) or TLX (clone 1, single cell clone, TLX^{+}) were treated with either control siRNA (siCon) or siRNA against TLX (siTLX) for 48 h. **A** mRNA expression of TLX was confirmed by qPCR (representative experiment shown of two, N = 4 internal replicates/condition, experiment repeated twice with similar results). Expression is shown as fold change relative to TLX^{con} values. Data are expressed as mean ±SEM. Different letters denote statistical difference

($p < 0.05$, one-way ANOVA followed by Tukey's multiple comparisons test). **B** Principal Component Analysis (PCA) based on the RNA-Seq gene expression patterns. **C** Volcano plots displaying differential gene expression in the following two comparisons: TLX^+ vs. TLX^{con} and TLX^+ vs. TLX^+ + siTLX. The top 5 upregulated and downregulated genes (by fold-change) for which there was also patient prognostic data (Fig 7 & Supplemental Tables 3 & 4) are labeled on the plots. SERPINB2 was also labeled on the TLX^+ vs. TLX^+ + siTLX plot although it ranked #7 in this comparison. Y-axis represents $-Log_{10}FDR$ and X-axis represents Log_2 fold-change, where red dots are significantly altered genes, as defined by FDR < 0.01. Grey dots are all genes with FDR > 0.01. **D** Treatment of TLX^+ cells with siTLX recovered 1,326 (~58%) of differentially expressed genes. **E** Gene set enrichment analysis (GSEA) using the Hallmark Gene Set indicated that TLX expression was inversely correlated with expression of genes in the KRAS signaling pathway as well as genes associated with epithelial mesenchymal transition (EMT). FDR < 0.05. **F** Heatmaps displaying expression (Log Counts Per Million) of genes that contributed to GSEA enrichment. (For B-F, N = 3 internal replicates/condition). Heatmaps for other identified pathways are shown in Supplemental Fig. 5.

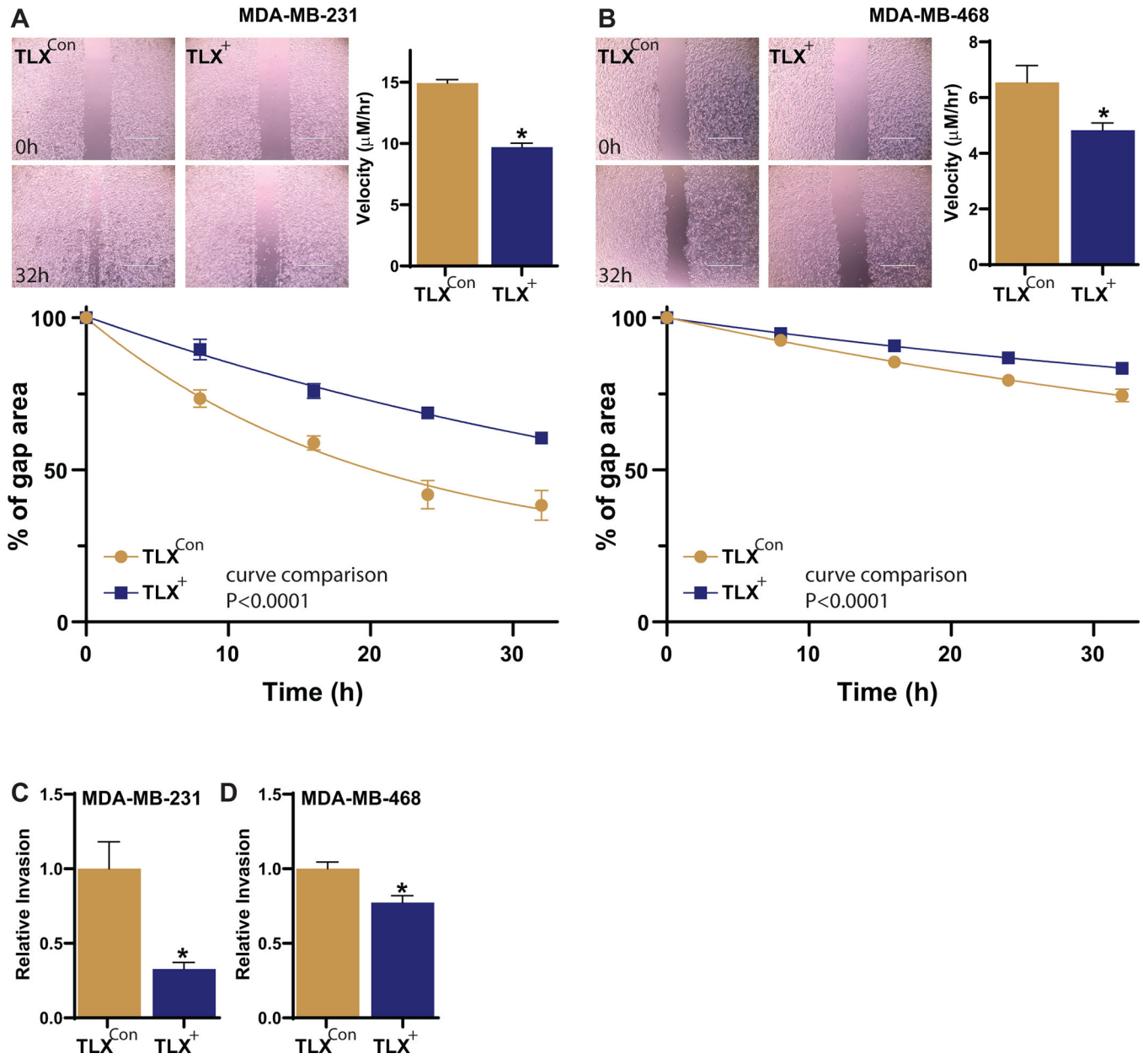

Figure 4. TLX impedes migration and invasion of cellular models of TNBC.

A & B Wound healing assays demonstrated that TLX^{+} reduced migration in (**A**) MDA-MB-231 cells (one representative experiment shown of three, N = 3 internal replicates/condition,) and (**B**) MDA-MB-468 cells (one representative experiment shown of three, N = 6/condition) compared to TLX^{con} cells. Representative images are to the left of quantified velocity bar graphs. Asterisks (*) indicate statistical significance ($p < 0.05$, student's unpaired two-tailed t test was performed). The lower graphs represent migration through time; one phase decay nonlinear regression was performed and resulting P value indicated. **C & D** Transwell invasion assays demonstrated that reduced invasion in (**C**) MDA-MB-231 cells (combined results of 3 independent experiments, N = 12 internal replicates/condition) and (**D**) MDA-MB-468 cells (combined results of 2 experiments N = 12 internal replicates/

condition) compared to TLX^{con} cells. Asterisks (*) indicate statistical significance ($p < 0.05$, student's unpaired two-tailed t test was performed). Data for this figure are expressed as mean ±SEM. Migration and invasion data from a second MDA-MB-231 clone (clone 2) are shown in Supplemental Fig. 6.

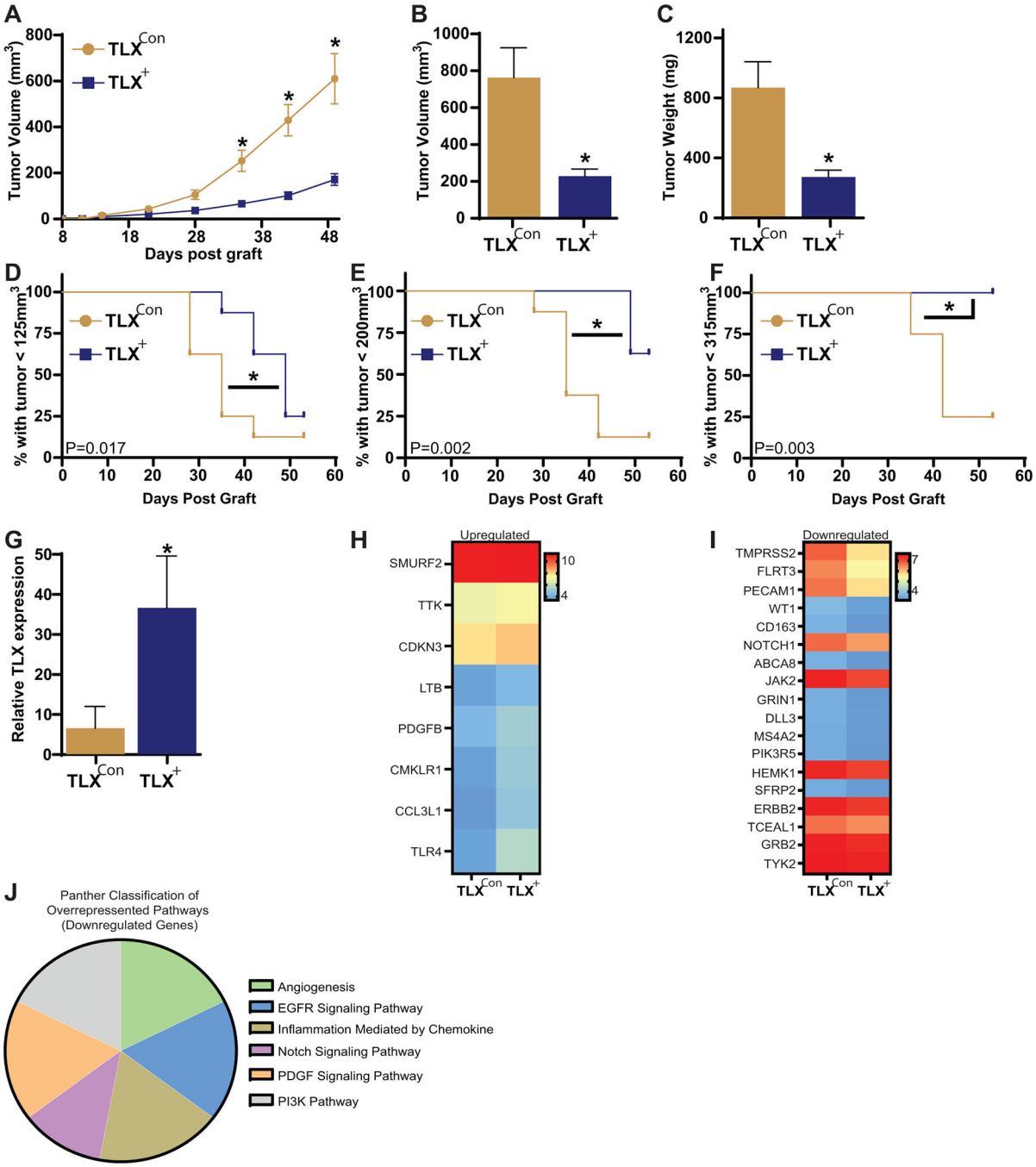

Figure 5. TLX impairs the growth of MDA-MB231 xenograft tumors, and regulates pathways associated with tumor progression.

Nude mice were orthotopically grafted with either TLX^{con} or TLX^{+} MDA-MB-231 cells (clone 1, N = 8/group). **A** Tumor volume through time, up to day 49, as measured by calipers. **B** Final tumor volume (one TLX^{con} mouse assessed at day 51, remainder assessed at day 53). **C** Final tumor weight at necropsy (one TLX^{con} mouse assessed at day 51, remainder assessed at day 53). **D-F** Kaplan-Meier plots assessing time to tumor volume endpoints of 125, 200 and 315mm^3 respectively. **G** TLX overexpression was maintained in

tumors, as assessed by qPCR. **H** RNA from MDA-MB-231 xenograft tumors (Supplemental Fig. 7) was analyzed on the Nanostring Breast Cancer 360 panel. Genes significantly upregulated in TLX^{+} compared to TLX^{con} tumors are depicted in **H**. **I** Genes significantly downregulated in TLX^{+} compared to TLX^{con} tumors. Data processing and analysis was done using the nSolver (Ver 4.0) software. Gene expression is represented as Log_2 counts. In-software t-test (Welch-Satterthwaite) was used to determine significant changes in gene expression ($P < 0.05$). **J** Differentially regulated genes identified in **H** and **I** were analyzed by the PANTHER Classification System. Only genes downregulated by TLX showed overrepresentation in associated pathways. Pie chart indicates percentage of downregulated genes associated with denoted pathway. Data for A-C and G are expressed as mean ±SEM. For A: two-way ANOVA followed by Sidak's multiple comparison test was performed, with asterisks (*) indicating significant differences between groups at the indicated time points. For B, C and G: student's unpaired two-tailed t test was performed with asterisks (*) indicating significant differences between groups. For G, data was Ln transformed prior to statistical testing. For D-F: the Gehan-Breslow-Wilcoxon test was performed. Statistical significant differences were considered if $p < 0.05$.

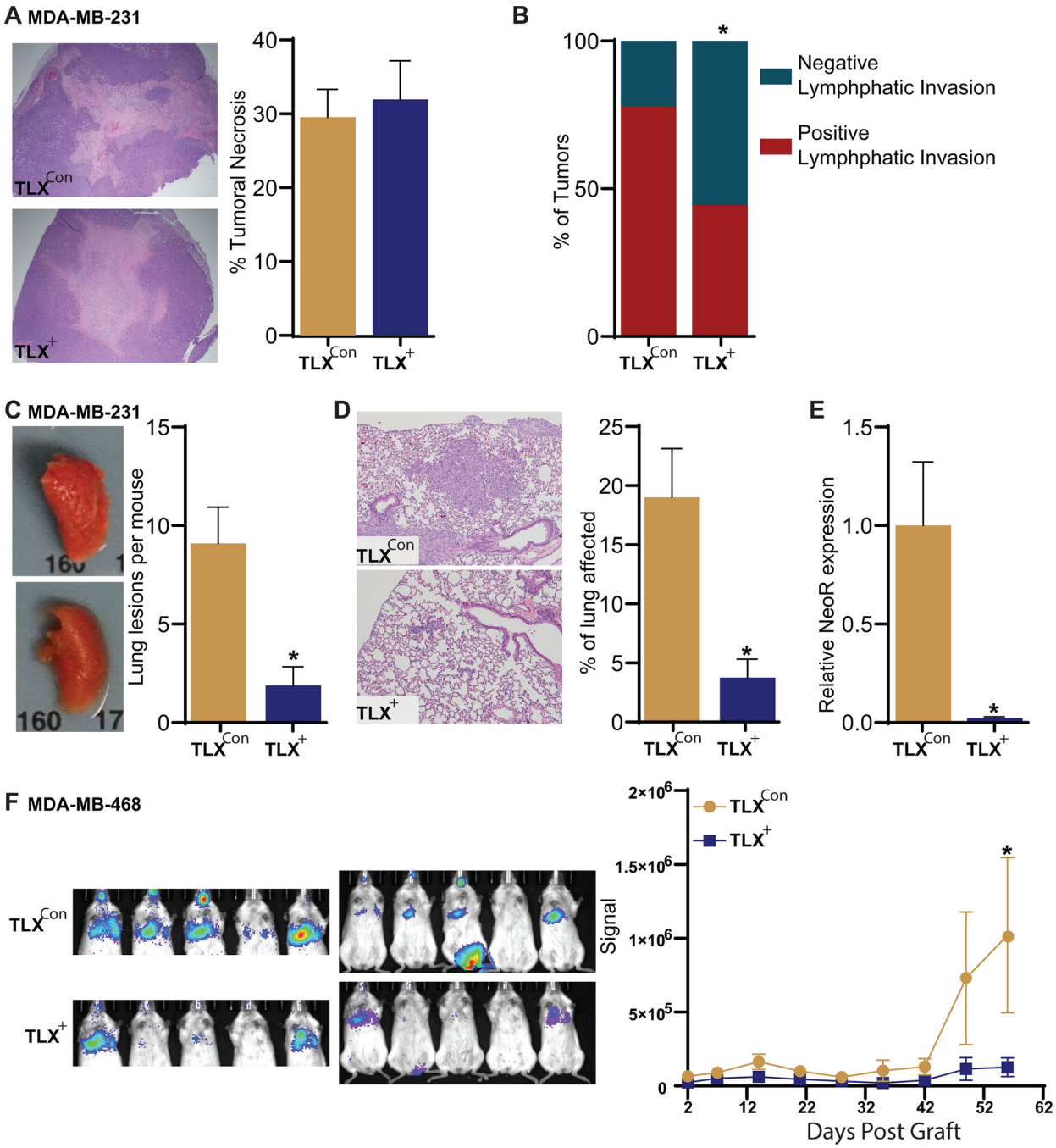

Figure 6. TLX decreases invasion and metastatic colonization *in vivo*.

A-B Histopathologic examination of tumors from MDA-MB-231 xenograft studies depicted in Fig. 5 and Supplemental Fig. 7. **A** Hematoxylin and eosin staining revealed no significant difference in tumoral necrosis between TLX^{con} and TLX^{+} tumor. Representative micrographs are to the left of quantified data **B** Lymphatic involvement, as assessed by a board-certified veterinary pathologist, was more likely to be observed in TLX^{con} tumors compared to TLX^{+} tumors. Chi-square test was performed, $P < 0.05$. **C-F** TLX^{con} cells had increased metastatic colonization and/or outgrowth compared to TLX^{+} cells in an

intravenous model of lung metastatic colonization. **C** Nude mice were grafted intravenously with MDA-MB-231 cells (N = 10 & 8 for TLX^{con} and TLX^{+}, respectively). Representative images of lungs are to the left of quantified data indicating that TLX^{+} cells resulted in fewer macroscopic lesions. **D** Representative micrographs of metastatic lungs are to the left of quantified data. **E** Expression of NeoR within metastatic lungs was quantified by qPCR, indicating the metastatic burden was lower in mice grafted with TLX^{+} cells. **F** NSG mice were grafted intravenously with MDA-MB-468 cells engineered to express luciferase (N = 10/group). Bioluminescence was followed through time. Representative images of the upper torso and full body are to the left of quantified data (upper torso). Data for A and C-F are mean ±SEM, and either a two tailed unpaired Student's t test, or two-way ANOVA followed by Sidak's multiple comparison test were used to determine statistical significance, which is indicated by an asterisk (*, $P < 0.05$).

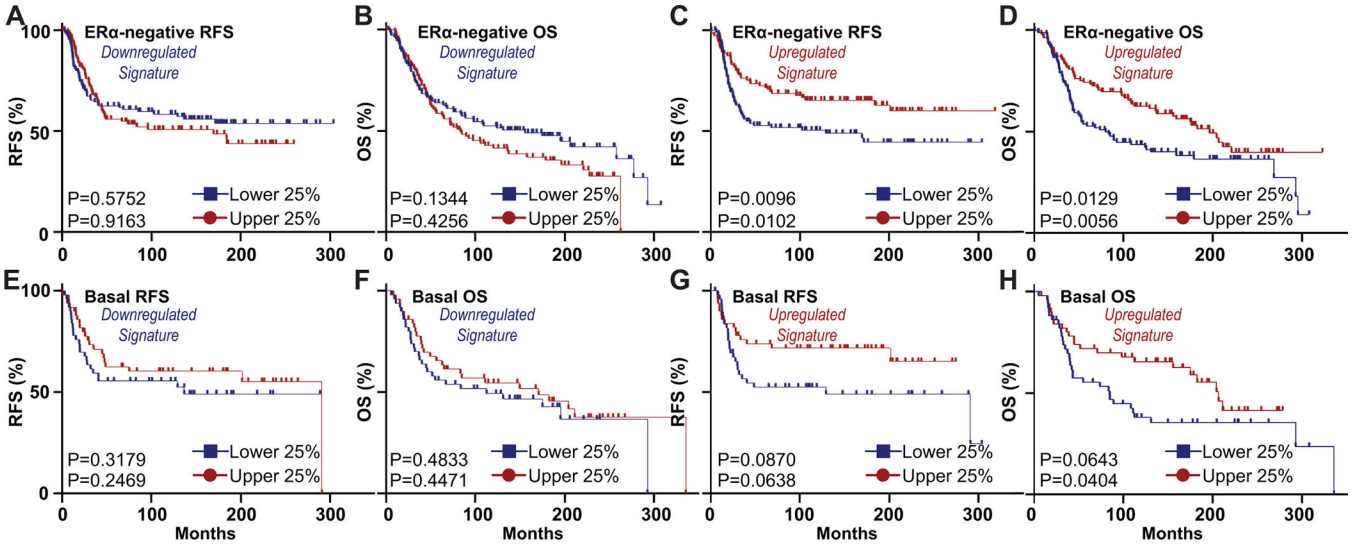

Figure 7. "TLX-upregulated gene signature" is positively correlated with survival.

Using the METABRIC data set, ERα-negative (**A-D**, N = 223) and basal (**E-F**, N = 100) patients were parsed into high (top 25%) and low (bottom 25%) cohorts for the "TLX-downregulated" and "TLX-upregulated" gene signatures. For this analysis, we weighted each gene in the signature equally. **A-D** The TLX-upregulated gene signature was correlated with significantly improved recurrence free survival (RFS) and overall survival (OS) in patients with ERα-negative disease. **E-H** Although slightly underpowered, similar findings were found for patients with basal tumors. Kaplan-Meier analysis followed by both the log rank test (top p-value on graph) and the Gehan-Breslow-Wilcoxon test (bottom p-value on graph) were performed.

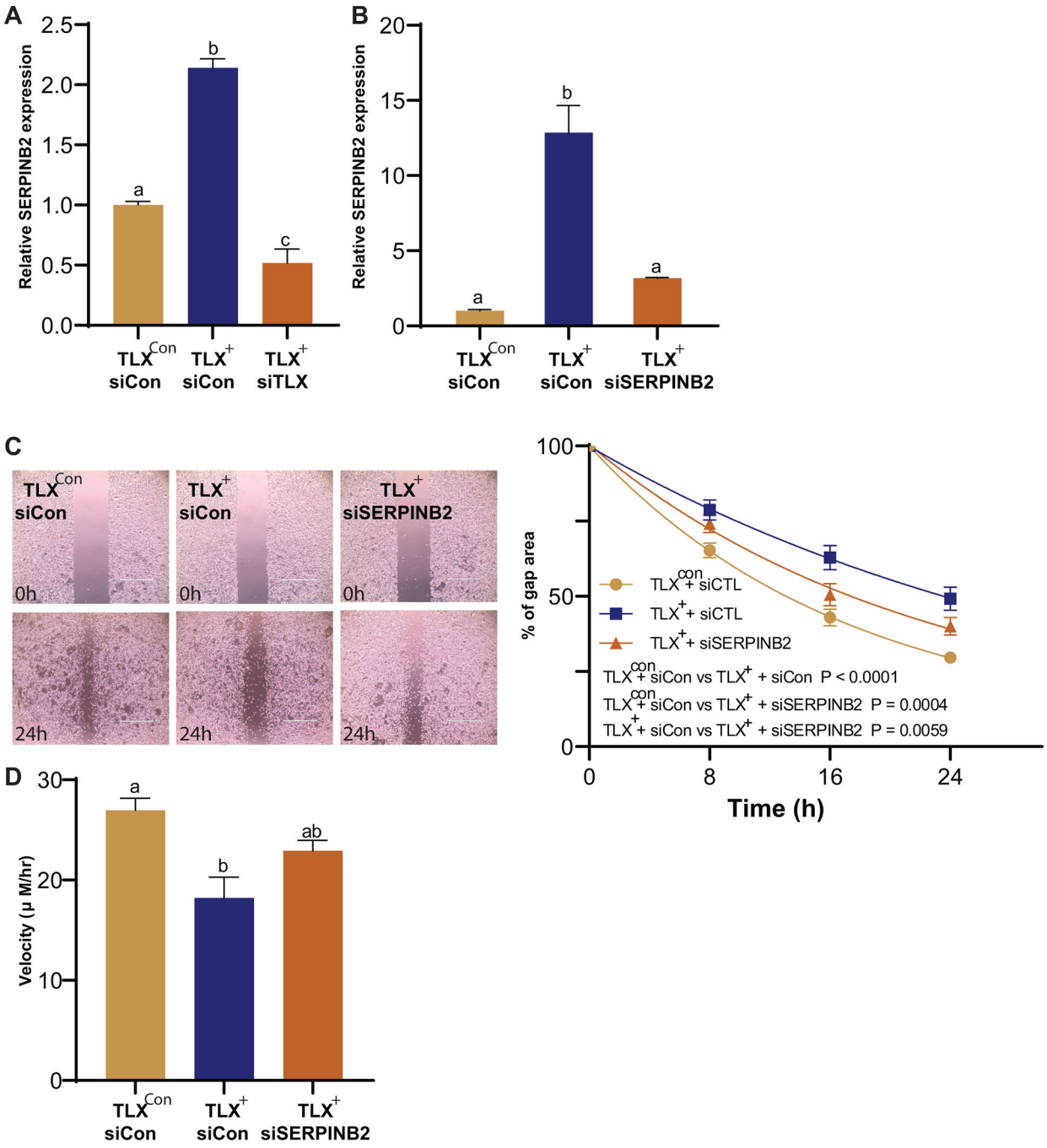

Figure 8. SERPINB2 required for anti-migratory effects of TLX.

A Expression of SERPINB2 is increased in MDA-MB-231 cells stably expressing TLX (TLX^+, clone 1) compared to a control empty vector (TLX^{con}), which can be recovered by treatment with siTLX. Results from a second clone and a second siRNA targeting TLX are demonstrated in Supplemental Fig. 9. **B** siRNA against SERPINB2 reduces its expression in TLX^+ cells (**A,** one representative experiment of two, N = 4 internal replicates/condition, **B**, representative experiment of three, N = 3 internal replicates/condition. qPCR analysis, expression is shown as fold change relative to TLX^{con} values). **C** Wound healing assays

(combined results of 3 experiments, N = 9 internal replicates/condition) demonstrate that TLX^+ cells treated with siSERPINB2 significantly increased gap closure rate compared to TLX^+ cells treated with siCont. Representative images are to the left of graph displaying migration through time (one phase decay nonlinear regression was performed and resulting P values indicated). **D** Knockdown of SERPINB2 in TLX^+ cells results in migration velocity between that of TLX^{con} and TLX^+ cells. Data are expressed as mean ±SEM unless otherwise indicated, different letters denote statistical difference ($p < 0.05$, one-way ANOVA followed by Tukey's multiple comparisons test).